SATURATION MUTAGENESIS OF TOLUENE/*o*-XYLENE MONOOXYGENASE AT ALPHA SUBUNIT RESIDUES F176, F196 AND Q204 FOR THE REGIOSPECIFIC HYDROXYLATION OF AROMATICS

by

Burcu SÖNMEZ

A thesis submitted to

the Graduate School of Sciences and Engineering

of

Fatih University

in partial fulfillment of the requirements for the degree of

Master of Science

in

Genetics and Bioengineering

January 2013
Istanbul, Turkey

APPROVAL PAGE

This is to certify that I have read this thesis written by Burcu SÖNMEZ and that in my opinion it is fully adequate, in scope and quality, as a thesis for the degree of Master of Science in Genetics and Bioengineering.

_____
Assist. Prof. Gönül SCHARA
Thesis Supervisor

I certify that this thesis satisfies all the requirements as a thesis for the degree of Master of Science in Genetics and Bioengineering.

_____
Prof. Dr. Halil Rıdvan ÖZ
Head of Department

Examining Committee Members

Assist. Prof. Gönül SCHARA _____

Assoc. Prof. Didem AKÇA GÜVEN _____

Assoc. Prof. M. Fatih ABASIYANIK _____

It is approved that this thesis has been written in compliance with the formatting rules laid down by the Graduate School of Sciences and Engineering.

_____
Assoc. Prof. Nurullah ARSLAN
Director

January 2013

SATURATION MUTAGENESIS OF TOLUENE/*o*-XYLENE MONOOXYGENASE AT ALPHA SUBUNIT RESIDUES F176, F196 AND Q204 FOR THE REGIOSPECIFIC HYDROXYLATION OF AROMATICS

Burcu SÖNMEZ

M.S. Thesis – Genetics and Bioengineering
January 2013

Thesis Supervisor: Assist. Prof. Gönül SCHARA

ABSTRACT

Toluene/*o*-xylene monooxygenase (ToMO) (EC: 1.14.13) is a multicomponent non-heme diiron enzyme with a broad substrate range of aromatics, including substituted benzenes. It has catalytic potentials for bioremediation of organic pollutants and synthesis of industrially valuable chemicals. In this study F176, F196 and Q204 positions of ToMO hydroxylase component (TouA) were subjected to site-saturation mutagenesis to investigate their roles in catalytic activity and oxidation regiospecificity. Site-saturation mutagenesis was achieved by overlap-extension PCR method and the mutants were screened using a rapid agar-plate assay. The isolated mutants were assayed by whole-cell biotransformation of phenol, toluene and naphthalene. Products were analyzed via high-pressure liquid chromatography. This study yielded two new regiospecific mutants of TouA F176 (F176N and F176H). TouA F176N variant was the most regiospecific mutant for hydroquinone formation (77%) from phenol and *p*-cresol formation (92%) from toluene. TouA F176H variant was also found to be an improved mutant for the tested substrates. For example, TouA F176H produces hydroxyphenol(s) 5-fold faster than wild-type ToMO (5.84 and 1.17 nmol/min·mg protein) from phenol. In addition, slight changes in regiospecificity were found among variants of TouA F196 and Q204. For example, TouA F196I variant produced 2-fold less *o*-cresol and 19% more *p*-cresol from toluene, and TouA Q204A variant produced 6% more 1-naphthol from naphthalene compared to wild-type ToMO.

Keywords: Toluene/*o*-xylene monooxygenase, site-saturation mutagenesis, aromatic hydroxylation.

TOLUEN/*o*-KSİLEN MONOOKSİJENAZIN ALFA ALTBİRİM F176, F196 VE Q204 POZİSYONLARIRININ AROMATİKLERİN REGİOSPESİFİK HİDROKSİLASYONU İÇİN SATURASYON MUTAGENEZİ

Burcu SÖNMEZ

Yüksek Lisans Tezi – Genetik ve Biyomühendislik
Ocak 2013

Tez Danışmanı: Yard. Doç. Gönül SCHARA

ÖZ

Toluen/*o*-ksilen monooksijenaz (ToMO) (EC: 1.14.13), sübstitue benzenleri de içeren geniş bir substrat yelpazesine sahip, çok-komponentli, hem-içermeyen, çift demirli bir enzimdir. Bu enzim, organik kirleticilerin biyoremediasyonu ve endüstriyel açıdan değerli olan kimyasalların sentezi için katalitik potansiyellere sahiptir. Bu çalışmada, ToMO hidroksilaz komponentinin F176, F196 ve Q204 pozisyonlarına katalitik aktivite ve regiospesifiklik üzerindeki etkilerini araştırmak amacıyla bölge saturasyon mutagenezi uygulandı. Bölge saturasyon mutagenezi "overlap-extension PCR" yöntemiyle gerçekleştirildi ve mutantlar hızlı bir agar-plak yöntemi ile tarandı. Elde edilen mutantlar ile fenol, toluen ve naftalin üzerinde tüm-hücre biyodönüşüm deneyleri yapıldı. Ürünler, yüksek basınç sıvı kromatografisi ile analiz edildi. Bu çalışma sonucunda, TouA F176 pozisyonu için iki yeni regiospesifik mutant (F176N ve F176H) elde edildi. TouA F176N mutantı, fenolden % 77 hidrokinon ve toluenden % 92 *p*-kresol elde ederek en regiospesifik mutant olarak tespit edildi. TouA F176H mutantı test edilen substratlar için aktivite artışı gösterdi. Örneğin, TouA F176H fenolden hidroksifenolleri yapan-tip ToMO'ya kıyasla 5 kat daha hızlı üretti (5.84 ve 1.17 nmol / dk · mg protein). Ayrıca, TouA F196 ve Q204 mutantlarından bazılarında küçük regiospesifik değişiklikler bulundu. Örneğin, wild-type enzime kıyaslandığında, TouA F196I mutantının, toluenden iki kat daha az *o*-kresol ve % 19 daha fazla *p*-kresol ürettiği, TouA Q204A mutantının ise naftalinden % 6 daha fazla 1-naftol ürettiği tespit edildi.

Anahtar Kelimeler: Toluen/*o*-ksilene monooksijenaz, bölge saturasyon mutagenezi, aromatik hidroksilasyonu.

To

my mother and father,

Emire and İbrahim Sönmez

ACKNOWLEDGEMENT

I would like to express my sincere gratitude to my supervisor, Assist. Prof. Gönül SCHARA, for her inspiring and thoughtful guidance and constant support. It was a great opportunity for me to be a member of her research group.

I would like to thank my thesis committee, Assoc. Prof. Didem AKÇA GÜVEN and Assoc. Prof. M. Fatih ABASIYANIK, and also to the head of department, Prof. Halil Rıdvan ÖZ.

I would like to give special thanks to my friends and lab mates, K. Cansu YANIK, Cansu KURT and Nurcan VARDAR for their cooperation, help and friendship. I also want to thank our research assistants, Umidahan DJAKBAROVA, Zeynep AYDIN, Bağdeser AKDOĞAN for their help and support. I also thank Esra YALÇIN and Büşra AYDOĞDU for their help in preparing SDS-gels.

I would to thank Environmental Engineering Department at Fatih University for providing the HPLC equipment.

I would like to thank Fatih University for the scholarship and support of the research project.

I wish to say big thanks to all my friends outside of the institute; specially to Dilek ÖZDEMİR, Emine ÇELİK, Sena İZ, Nurdan BÜLBÜL, Sibel KURAL, Sevda AKAY, Fatime EREN for their encouragement, support and friendship.

My big special thanks go to my parents, my grandparents, my sister, my brother and his wife. I gratefully thank to my mother and father for their continuous love, patience, dedication and support.

TABLE OF CONTENTS

LIST OF TABLES

TABLE

LIST OF FIGURES

FIGURE

:

LIST OF SYMBOLS AND ABBREVIATIONS

SYMBOL/ABBREVIATION	
4NC	4-Nitrocatechol
A570	Absorbance at 570 nm
APS	Ammonium persulfate
ATSDR	Agency for Toxic Substances and Disease Registry
BMMs	Bacterial multicomponent monooxygenases
bp	Base pair
BSA	Bovine serum albumin
COMT	Catechol-*o*-methyltransferase
cis-DCE	*cis*-dichloroethylene
ddH_2O	Double distilled water
dNTPs	Deoxyribonucleotide triphosphate
E. coli	*Escherichia coli*
EPA	Environmental Protection Agency.
FAD	Flavin Adenine Dinucleotide
Fe_A	Iron A
Fe_B	Iron B
Glu	Glutamate
H_3O^+	Hydronium
His	Histidine
HPLC	High performance liquid chromatography
hr	Hour
kDa	Kilodalton

LB	Luria-Bertani
mg	Miligram
min	Minute
ml	Mililiter
NADH	Nicotinamide adenine dinucleotide
NB	Nitrobenzene
ng	Nanogram
nm	Nanometer
OD	Optical density
PCE	Tetrachloroethylene
PCR	Polymerase chain reaction
p-NP	*p*-nitrophenol
rpm	Revolutions per minute
RT	Retention time
SDS	Sodium dodecyl sulfate
SDS-PAGE	Sodium dodecyl sulfate polyacrylamide gel electrophoresis
T4MO	Toluene 4-monooxygenase
TAE	Tris-acetate EDTA
TEMED	N, N, N', N'-tetramethylethylenediamine
TCE	Trichloroethylene
TMO	Toluene monooxygenase
TOM	Toluene *ortho*-monooxygenase
ToMO	Toluene *o*-xylene monooxygenase
TouA	α-hydroxylase of ToMO
TouB	γ –hydroxylase
TouC	Rieske type ferredoxin
TouD	Effector protein
TouE	β –hydroxylase
TouF	NADH ferredoxin oxidoreductase
TmoA	α-hydroxylase of T4MO
T*p*MO	Toluene *para*-monooxygenase
trans-DCE	*trans*-dichloroethylene

Tris-EDTA	Tris- Ethylenediaminetetraacetic acid
Tris-HNO_3	Tris-nitric acid
UV	Ultraviolet
Å	Armstrong
µl	Microliter
µM	Micromolar

CHAPTER 1

INTRODUCTION

1.1 TOLUENE MONOOXYGENASES (TMOs)

Toluene monooxygenases (TMOs) (EC: 1.14.13) are oxidoreductases which have the ability to oxidize a variety of aromatic compounds. The hydroxylation of aromatics requires molecular oxygen as the electron acceptor and protons in the form of H_3O^+ and produces water as by-product (McCormick and Lippard, 2012). TMOs are soluble, non-heme, dinuclear iron containing monooxygenases and have been classified into a family of four-component arene/alkene monooxygenase of bacterial multicomponent monooxygenases (BMMs) based on their natural substrates and gene sequence similarities (Notomista et al., 2003). Toluene monooxygenases exist in a variety of organisms. Toluene/*o*-xylene monooxygenase (ToMO) of *Pseudomonas sporium* (formerly *P. stutzeri*) OX1 is the subject of this thesis (Baggi et al., 1987, Radice et al., 2006). Other extensively studied toluene monooxygenases are toluene-4-monooxygenase (T4MO) of *Pseudomonas mendocina* KR1 (Yen et al., 1991), toluene-*para*-monooxygenase (T*p*MO) of *Ralstonia pickettii* PKO1 (Byrne et al., 1995) and toluene *ortho*-monooxygenase (TOM) of *Burkholderia cepacia* G4 (Newman and Wackett, 1995).

1.1.1 Toluene/*o*-Xylene Monooxygenase

Toluene/*o*-xylene monooxygenase is a multicomponent oxygenase system. The *tou* locus was cloned from the chromosome of *Psuedomonas sp.* OX1 and it expresses six open reading frames (*touABCDEF*) under the control of a single promoter (Cafaro et. al, 2005).

1.1.1.1 Structure

The components of ToMO have a high degree of sequence similarity with that of other monooxygenases (Bertoni et al., 1998). ToMO hydroxylase component (~220 kDa) is a subcomplex of TouA, TouB and TouE with a quaternary structure of $\alpha_2\beta_2\gamma_2$ (Figure 1.1). TouF is an NADH-oxidoreductase and TouC is a rieske-type protein. TouF shifts electrons from NADH via its FAD and [2Fe-2S] domains to TouC and electrons are finally transferred to hydroxylase component. TouD is a regulatory protein (Cafaro et al., 2002, Bailey et al., 2008). It is proposed that the regulatory protein shares a binding site with the reductase (TouF) on the hydroxylase component. Structural studies with a relative enzyme of ToMO suggests that binding of the regulatory protein blocks the access of the reductase to get near the active site to control the reduction of the dioxygen-activated diiron center and may cause conformational changes at channels (Bailey et al., 2008). Therefore, the interaction among hydroxylase, the regulatory protein and the reductase is in coordination with the oxidation state and conformation of the active site.

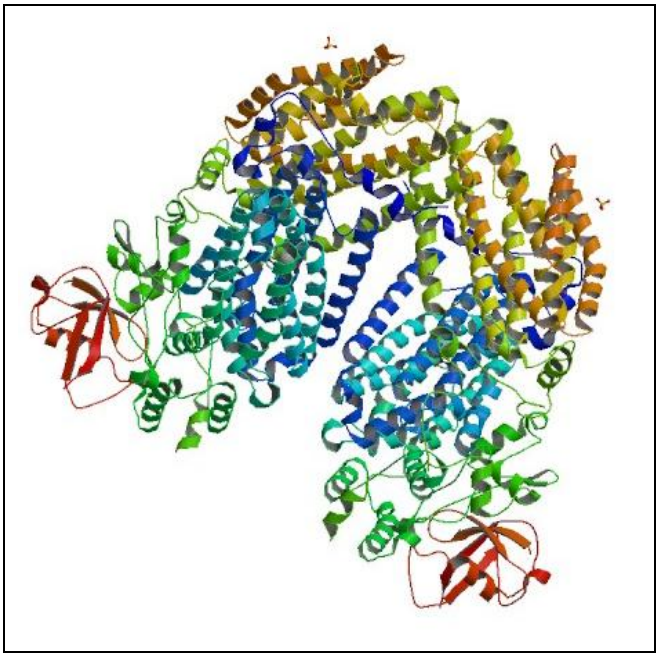

Figure 1.1 Global structure of toluene/*o*-xylene monooxygenase hydroxylase. It contains two α-subunits (blue/green), two β-subunits (yellow/orange), and two γ-subunits (red). Protein Data Bank (PDB) Entry: 1T0Q (Sazinsky et al., 2004).

Crystal structure of the ToMO hydroxylase has shown that there is a non-heme diiron catalytic center (Fe_A-Fe_B) located interiors of each alpha subunit. Dioxygen activation and subsequent substrate oxidation take place at the carboxylate-bridged diiron center. Fe_A is stabilized by coordinating residues Glu104, Glu134, His137 and Fe_B is stabilized by His234, Glu197, Glu231; and there is 3.0 Å distance between the two iron centers (Sazinsky et al., 2004). A Pymol (Schrödinger, LLC., 2010) image of the diiron center with its coordinating residues is shown in Figure 1.2.

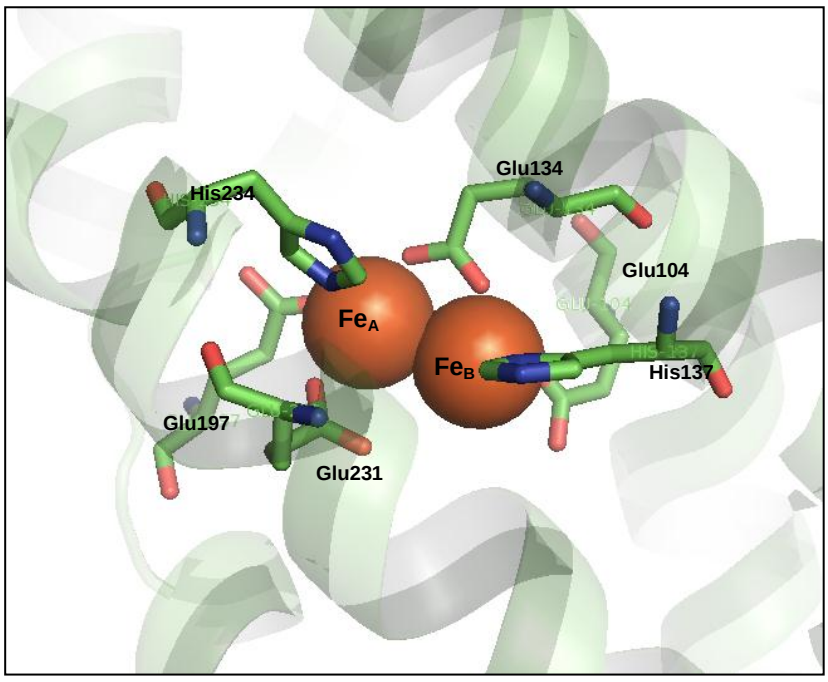

Figure 1.2 The diiron active site of ToMOH. Iron atoms are shown as spheres and the coordinating residues are shown as sticks. Carbon, nitrogen, oxygen, and iron atoms are colored green, blue, red, and orange, respectively.

The active site is connected to the surface of the protein through a large channel (35-40 Å in length and 6-10 Å in width) with a fork structure leading to two adjacent openings at the surface. It was postulated that this channel exposes the active center to bulk solvent and forms a route for the substrate to move in and the product to go out (Sazinsky et al., 2004). A structural study with T4MO hydroxylase with its respective regulatory protein conferred that the channel undergoes major conformational changes upon binding of the regulatory protein and it is closed down to limit the solvent access

to protect the active site intermediates (Murray and Lippard, 2007).

Besides the substrate channel, a divergent path is formed by a series of cavities which traverse alpha-subunit starting from the surface towards the diiron center. The substrate channel overlaps this path at the first cavity neighboring the active site (Figure 1.3). The surface of the cavities is constituted of mainly hydrophobic residues. Structural and mechanistic studies conferred that the hydrophobic cavities may provide a route for molecular oxygen transport to the diiron site (Song et al., 2011, McCormick and Lippard, 2012).

In addition to the channels, there is a pore pocket region that neighbors the diiron center (Figure 1.3). The surface of pore pocket region is constituted of conserved and flexible hydrophilic residues which allow conformational changes, make interaction with regulatory protein and contribute to accessibility of the active center. These residues are a threonine at 201th with critical role in the proton transfer to diiron center (Song et al. 2010), a flexible asparagine at 202nd position which can make hydrogen-bonding with regulatory protein, a surface glutamine at 228th position and an iron-coordinating glutamates at 231st positions (McCormick et al., 2006, Murray and Lippard, 2007, McCormick and Lippard, 2012).

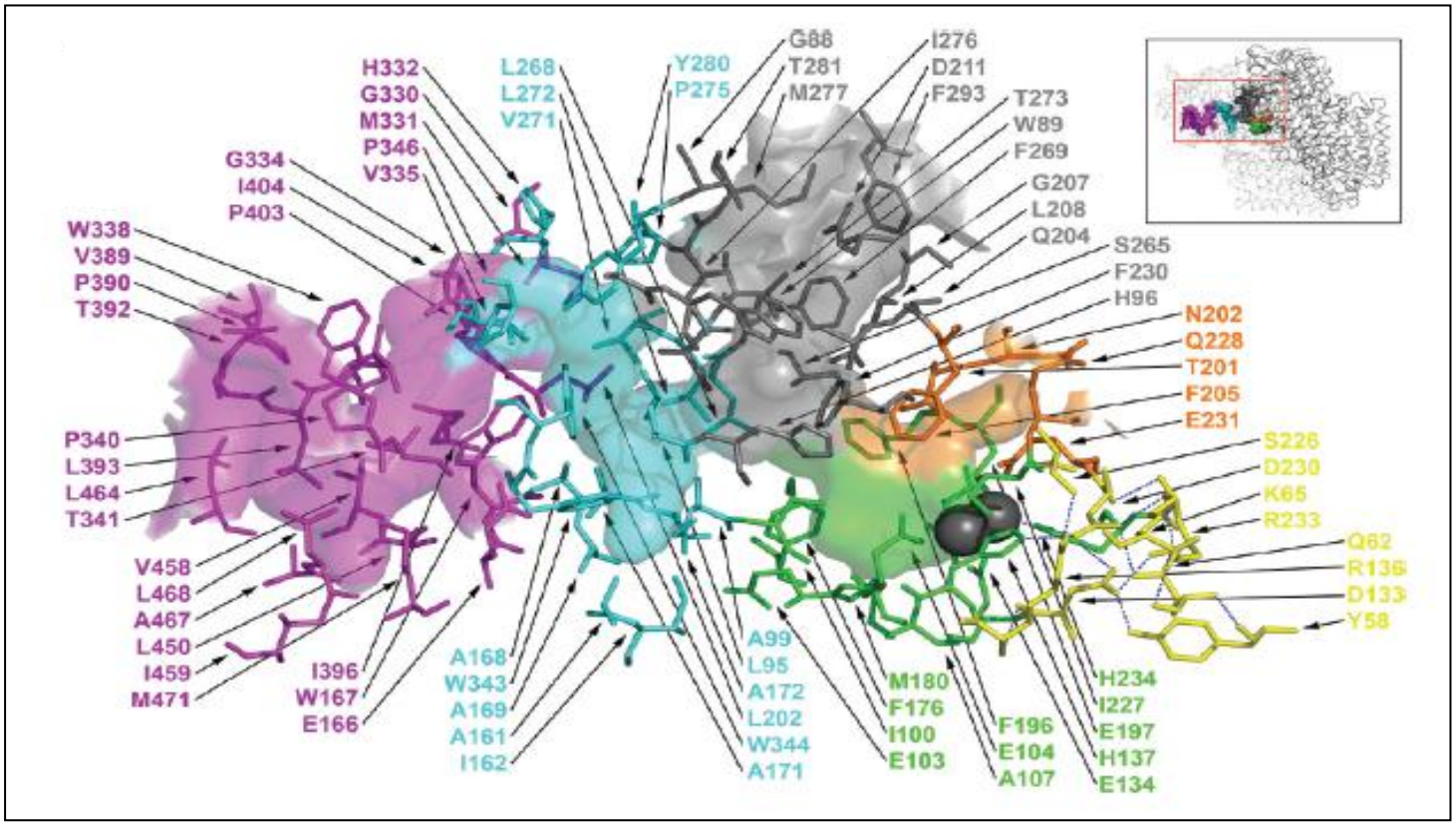

Figure 1.3 van der Waals surfaces and the contributing residues of cavity-1 (green), cavity-2 (cyan), cavity-3 (magenta), pore region (orange) and channel (gray) in the α-subunit of ToMOH. The yellow sticks represent the putative electron-transport hydrogen-bonding network residues (McCormick and Lippard, 2012).

1.1.1.2 Mechanism

Molecular oxygen activation and substrate hydroxylation occurs at the carboxylate-bridged diiron center located interior of the alpha-subunits of the ToMO hydroxylase component. According to the proposed mechanism, the iron atoms of the resting enzyme are at the reduced ferrous state (diiron [II]) (Figure 1.4). The catalytic cycle is initiated by the attack of diiron [II] on molecular oxygen and electrons are transferred to oxygen to generate a reactive peroxodiiron [III] intermediate (Song, 2011). Subsequently, the reactive oxygenated diiron core attacks on the aromatic ring of the substrate and hydroxylated product is liberated with the assistance of water, leaving the iron atoms at a resting ferric state (diiron [III]). For the start of another reaction cycle, the ferrous state diiron [II] must be regenerated by transferring two electrons from the reductase/Rieske protein components of ToMO (Song, 2011). According to a model by Bochevarov et. al, the peroxo intermediate may be in protonated form and stabilized by nearby threonine at 201st position (Bochevarov et al., 2011).

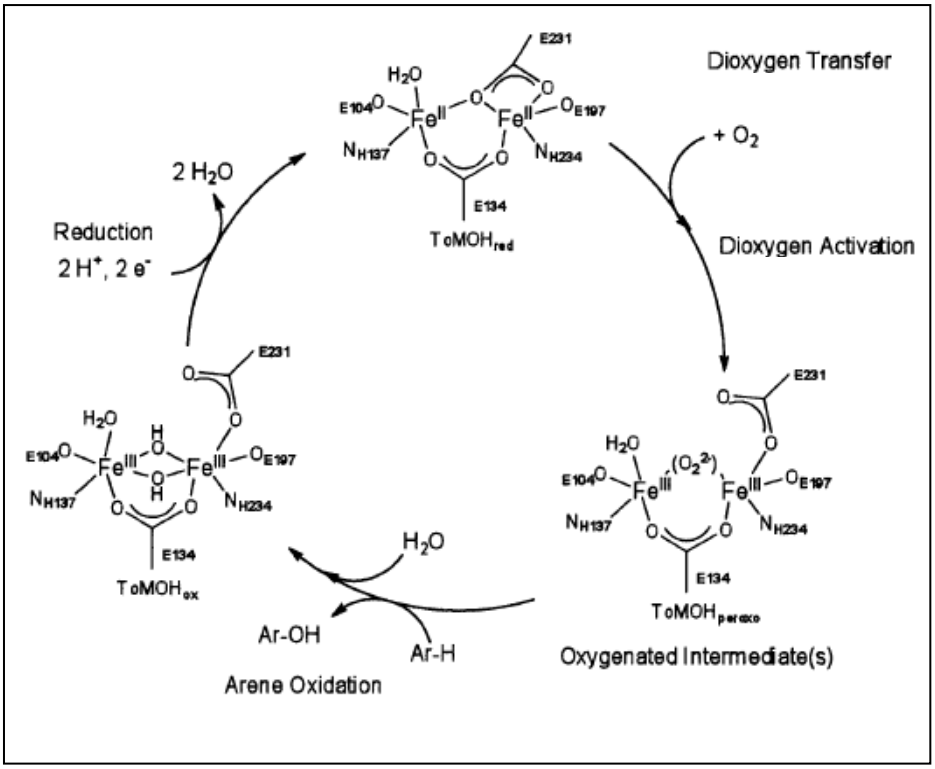

Figure 1.4. The catalytic cycle of ToMOH. Ar-H: Aromatic substrate; Ar-OH: the product. (Song, 2011).

1.2 TARGETED TouA POSITIONS

1.2.1 TouA Phenylalanine at 176

All the toluene monooxygenases have a phenylalanine at the respective position to the F176 of ToMO. It is located in the first cavity housing the diiron center and 4.3 Å away both from the gate residue I100 (Vardar and Wood, 2005b) and the substrate channel. Its distance from Fe_A and Fe_B is 8.8 Å and 8.6 Å away, respectively, according to the measurements on PyMOL (Figure 1.5).

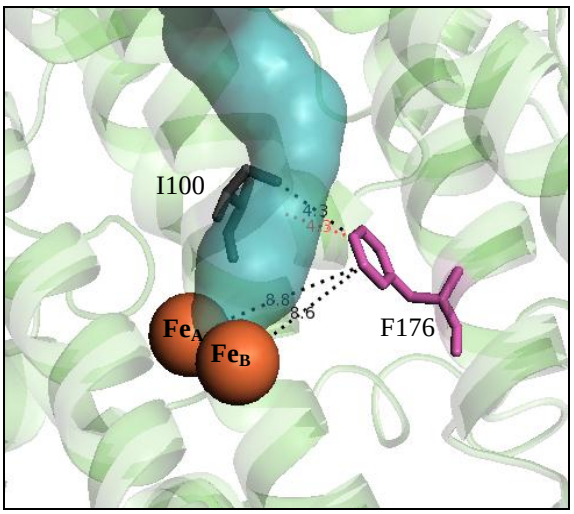

Figure 1.5 The positioning of TouA 176 (purple sticks) with respect to channel (cyan surface), the gate residue I100 (black sticks) and the iron atoms (orange spheres).

TouA F176 position has not been studied extensively by saturation mutagenesis before and there are few studies performed by rational design approach. Based on a computational model, TouA F176I, F176L and F176T single mutants and six E103G-F176X (X: I, L, T, A, S, V) double mutants were generated by site-directed mutagenesis (Notomista et al., 2009, Notomista et al., 2011). Mutants were tested for the oxidation of a non-natural substrate 2-phenylethanol. The single and double mutants showed different regiospecificity than the wild type, shifting from *meta* to *para* hydroxylation. Therefore, it was suggested that phenylalanine at position 176 causes steric hindrance and disturb the proper positioning of the reaction intermediate of the *para*-hydroxylated

product in the active site. Also, the double mutants showed enhanced catalytic activity towards 2-phenylethanol, among which E103G/F176T was the most improved one with around 13-fold increase in comparison to wild-type ToMO. In another study, the importance of this position for the activity was emphasized by showing that a T4MO TmoA F176A variant could not oxidize toluene, TCE, or butadiene, whereas a TmoA F176L variant retained 100% activity toward toluene with 25.5% and 38.4% activity toward TCE and butadiene (Sazinsky et al., 2004).

1.2.2 TouA Phenylalanine at 196

All toluene monooxygenases have a phenylalanine at the corresponding position of the F196 of ToMO. It is located in the active site pocket and 5.8 Å away from the gate residue I100 and 3.4 Å from the substrate channel. Its distance from Fe_A and Fe_B is 8.0 Å and 7.0 Å away, respectively, according to the measurements on PyMOL (Figure 1.6).

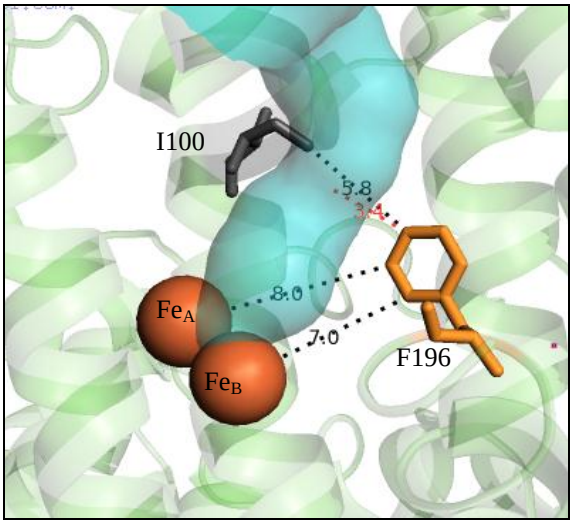

Figure 1.6 The positioning of TouA F196 (orange sticks) with respect to channel (cyan surface), the gate residue I100 (black sticks) and the iron atoms (orange spheres).

The role of F196 on ToMO activity has not been studied before. However, McClay et al. studied the analog of this residue on T4MO for the regiospecific indole oxidation. By using site-directed mutagenesis, they generated TmoA F196L, F196Y and

F196I substitutions, which are conservative mutations. The variant F196L exhibited a significant change in product distribution; suggesting that this position may have a role in the regiospecificity of indole oxidation (McClay et al., 2005).

1.2.3 TouA Glutamine at 204

All toluene monooxygenases have a glutamine at the respective position to the Q204 of ToMO, except TOM has a leucine with an aliphatic side chain. It is located on the substrate channel. It is 6.7 Å away from I100 and 3.6 Å from substrate channel. Its distance from Fe_A and Fe_B is 10.2 Å and 10.7 Å away, respectively, according to the measurements on PyMOL (Figure 1.7). The role of this position on the catalytic activity of ToMO or any other toluene monooxygenase has not been studied before.

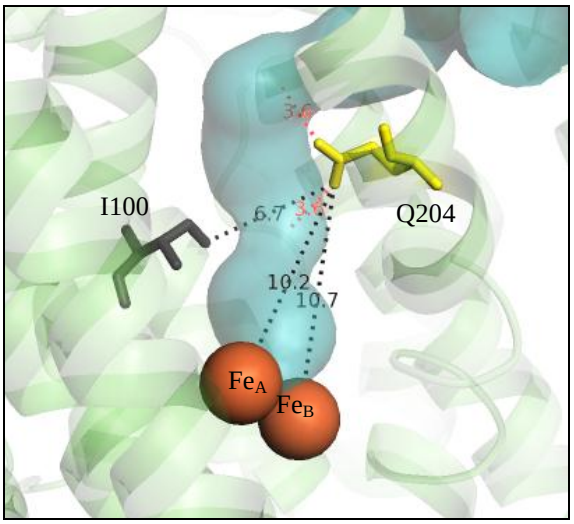

Figure 1.7 The positioning of TouA Q204 (yellow sticks) with respect to channel (cyan surface), the gate residue I100 (black sticks) and the iron atoms (orange spheres).

1.3 IMPORTANCE OF TOLUENE MONOOXYGENASES

The recombinant constructs of four toluene monooxygenases, T4MO, T*p*MO, TOM and ToMO, have been previously expressed in *Escherichia coli* TG1 to study their catalytic features. Toluene monooxygenases possess biotechnological potentials in the manufacture of chemical intermediates, organic synthesis or the detoxification of pollutants. Toluene monooxygenases have differences in their substrate preferences and

degree of regiospecificity. There is an ongoing interest in understanding the key structural determinants of the catalytic properties of these enzymes (Fishman et al., 2006).

1.3.1 Biocatalysis

Biocatalysis is the use of enzymes, either as pure or whole-cell, in chemical reactions. The impact of biocatalysis in the industry is growing. It is estimated that biocatalysis would be involved in the production of at least 20% of global chemicals by 2020 (Meyer and Turner, 2009). There is an increasing demand for more clean and economic processes. Biocatalysis has several advantageous over traditional chemical synthesis. It can be more economic and environmentally benign. It can be carried out with less organic solvents, under milder conditions and it is a more selective process which increases product yield with lesser by-products and waste. What is more, it can be even the sole method to produce a certain compound (de Carvalho, 2011).

TMOs have been shown to be useful biocatalysts for organic synthesis. TMOs are capable of three successive hydroxylation of benzene; it means they produce phenol, catechol and trihydroxybenzenes step by step (Tao et al., 2004b). The first product of this conversion, phenol, is a chemical intermediate in the production of phenolic resins, which are used in several industries such as plywood, construction and automotive; also used in the synthesis of intermediates and in the production of nylon and epoxy resins (ATSDR, 1998). Catechol production is also a very important feature; this compound and its derivatives are used in pharmaceutical industry, in textile industry for processing fur dyes and also as a chemical intermediate for antioxidants in rubber and greasers (EPA, 2007).

TMOs can catalyze successive hydroxylation of toluene. They show differences in the degree of regiospecificity in toluene hydroxylation. ToMO has the ability to catalyze three distinct regiospecific hydroxylation of toluene to produce *o*-, *m*-, and *p*-cresol (Vardar and Wood, 2005b). While T4MO and T*p*MO produce *m*- and *p*-cresols, TOM produces *o*-cresol exclusively (Rui et al., 2004, Tao et al., 2004a, Fishman et al., 2005) ToMO was reported to produce both 3- and 4-methylcatechols from cresols in the second hydroxylation step (Vardar and Wood, 2004). The resultant cresols and substituted catechols are useful products. *o*-Cresol is used as a solvent and disinfectant,

m-cresol is used to produce agrochemicals and to produce antioxidants and the major use of *p*-cresol is for the manufacture of antioxidants and the fragrance (ATSDR, 2008). Methylcatechols are also important intermediates for food and pharmaceutical industries (Fishman et al., 2006).

Naphthalene is a polycyclic organic compound which has two fused aromatic rings. It has been shown that TOM produces only 1-naphthol from naphthalene oxidation, while ToMO, along with T4MO and T*p*MO produces 2-naphthol as well (Tao et al., 2005). Large quantities of naphthols are used in the industry for the manufacture of organic intermediates for dyes, pharmaceuticals, perfumes, surfactants, and agrochemicals (Raynaudlacroze and Tavare, 1993).

TMOs oxidize nitrobenzene to produce *m*- and *p*-nitrophenol, and it was also reported that ToMO can oxidize *m*- and *p*-nitrophenol to produce 4-nitrocatechol and oxidize *o*-nitrophenol to 3-nitrocatechol and nitrohydroquinone (Vardar, et al., 2005b). Dihydroxy-derivatives of nitrobenzene are useful compounds in pharmaceutical industry. Nitrocatechols are used in the synthesis of catechol-o-methyltransferase (COMT) inhibitors for use in the treatment of Parkinson's disease (Palma et al., 2003, Bonifacio et al., 2007) and have potentials as competitive inhibitors of neural nitric oxide synthase which is associated to pathology of Parkinsons disease (Palumbo et al., 2002).

1.3.2 Bioremediation

Chemical compounds have been released and accumulated in the environment as a result of large-scale of manufacture and insufficiency in the treatment of wastes and disposal methods (Chen et al., 1999). The pollution causes disturbance of the natural balance of the ecosystem and pose health risks for organisms.

Benzene and its substituted derivatives are ubiquitous pollutants in the environment (Mithaishvili et al., 2005). They are produced in large amounts for their use in commercial areas and they are health threatening chemicals. For example, benzene is listed as a known human carcinogen by US Environmental Protection Agency (EPA). It is used as an ingredient in motor fuels; as a solvent in the manufacture of fats, resins, oils, paints, plastics, and rubber; it is also applied in food industry in the

process of oil extraction from seeds and used as a chemical intermediate in the production of detergents and pharmaceuticals (ATSDR, 2007). Nitrobenzene is a volatile organic compound and an anticipated human carcinogen. It is primarily used in organic synthesis and also used in the production of rubber, agrochemicals and pharmaceuticals (ATSDR, 1990). Toluene is primarily used as a constituent in gasoline to improve its octane rating. It is also a widely used solvent in several products such as paintings, cosmetic nail polishes, synthetic fragrances and adhesives. It is a toxic chemical which affects primarily central nervous system in humans upon short- or long-term exposure (ATSDR, 2000).

Conventional remediation approaches to deal with pollution include excavation, chemical treatment and thermal treatment. These methods are generally expensive, inefficient and prone to generation of harmful by-products and secondary pollution (Vidali, 2001). Therefore, development of alternative remediation strategies has become an area of interest. Bioremediation is a new technology for the clean-up of contaminated sites. This approach has several advantages over traditional methods. It is a natural process and usually does not generate harmful by-products. It can be cost-effective and can also achieve complete mineralization of the contaminants (Wood, 2008).

Bioremediation relies on the presence of suitable microorganism which expresses the enzymes that catalyze the conversion of wastes. It utilizes the ability of microorganisms to metabolize pollutants as a carbon and energy source, whilst degrading them into non- or less-toxic substances. The oxidation of benzene ring is the first step in anaerobic metabolism of the aromatic pollutants. Consequently, substituted phenols are further metabolized by catabolic enzymes in the repertoire of organisms and eventually metabolites are converted to citric acid cycle intermediates (Bouwer and Zehnder, 1993). Toluene monooxygenases have potentials of applicability in bioremediation due to their ability to oxidize various aromatics, including benzene, nitrobenzene, toluene and their derivatives. In fact, toluene monooxygenase genes are associated to biodegradation of petroleum hydrocarbons at contaminated sites (Ma and Herson, 2000, Baldwin et al., 2009, Nebe et al., 2009). An Antarctic bacterium has been engineered to express recombinant ToMO to enable it to grow on aromatics as a sole carbon energy source and hence, to be used in bioremediation of contaminated marine environments and/or cold industrial effluents (Siani et al., 2006).

Chlorinated ethenes, including perchloroethene (PCE) and trichlorethene (TCE) are among the major groundwater pollutants at hazardous waste sites. PCE is the main chemical solvent applied in dry cleaning and TCE is primarily used in metal degreasing and in textile industry. Both are possible human carcinogens and other chlorinated solvents are also pose health hazards. Microbial degradation of this group of chemicals can occur both aerobically and anaerobically. However, anaerobic dehalogenation of chlorinated ethenes is incomplete and generates toxic and possible carcinogenic reaction intermediates (Alvarez-Cohen and McCarty, 1991). On the other hand aerobic degradation can achieve complete mineralization (Bradley and Chapelle, 1998, Chauhan et al., 1998). Toluene monooxygenases possess the activity of chlorinated ethene oxidation individually and as in mixtures (Shim and Wood, 2000). ToMO is the only known enzyme which is capable of PCE oxidation, besides, its expression in *Pseudomonas sp.* OX1 is induced by TCE and PCE and this organism is chemotactic towards chlorinated aliphatics (Ryoo et al., 2000, Ryoo et al., 2001, Shim et al., 2001, Vardar et al.,2005a).

1.4 PROTEIN ENGINEERING

Enzymes have several characteristics that make them more powerful than conventional catalysts for several industrial chemical syntheses. Enzymes exhibit high chemo-, regio-, and stereoselectivity. Besides, thank to progresses in DNA technology, many enzymes are produced at a commercial scale and economically (Bornscheuer and Pohl, 2001). Enzymes are utilized in the manufacture of over 500 products for a broad range of application (Rubin-Pitel and Zhao, 2006). However, the industrial process conditions are not always appropriate for the chemistry of natural enzymes. Protein engineering has been applied to tailor enzymes to overcome the process limitations and yield biocatalysts with higher activity, specificity and stability at a given condition (Bommarius et al., 2011). In addition, it can be applied to engineer enzymes which have new capabilities such as activity towards non-natural substrates or catalysis of novel reactions (Bornscheuer et al., 2012). Protein engineering strategies can be broadly divided into two; rational design and directed evolution (Bornscheuer and Pohl, 2001).

1.4.1 Rational Design

Rational design requires detailed knowledge of enzyme structure, function and mechanism to predict beneficial mutations to create the structural changes that lead to the desired properties. The mutations are introduced by site-directed mutagenesis, a PCR-based method that employs mutagenic oligonucleotides (Bornscheuer and Pohl, 2001). When the structural information is not available, computational modeling tools are used to build homology models based on sequence similarity to related proteins with known structures. This approach has been used to understand the basis for the characteristic nitroarene specificity of nitrobenzene 1, 2-dioxygenase from *Comamonas sp.* strain JS765 (Ju and Parales, 2006) and to change the regioselectivity of P450 BM-3 monooxygenase from *Bacillus megaterium* (Dietrich et al., 2009).

In rational design, creation of desired mutants is fast and easy. The targeted sequence space is small and this eliminates the need of screening large numbers of mutant libraries. However, the precise identification of the key amino acids requires high-quality structures or models, and the success is hindered by the limited understanding of the enzyme structure/function relationships. Besides, single substitutions may not be sufficient to obtain comprehensive knowledge, since there is 19 amino acid substitutions possible for any single position to be investigated (Chica et. al., 2005).

1.4.2 Directed Evolution

In contrast to rational design, directed evolution does not require prior knowledge of structure or mechanism. This approach can be simply described as employment of repeated cycles of molecular evolution in a laboratory (Arnold, 1997) (Figure 1.8). The strategy involves generation of a mutant population with sufficient gene diversity for the given function and then, selection of the improved variants. The diversity is generally achieved by random mutagenesis and/or in vitro recombination of gene fragments and identification of improved variants is done by high-throughput screening or selection systems (Zhao et al, 2002).

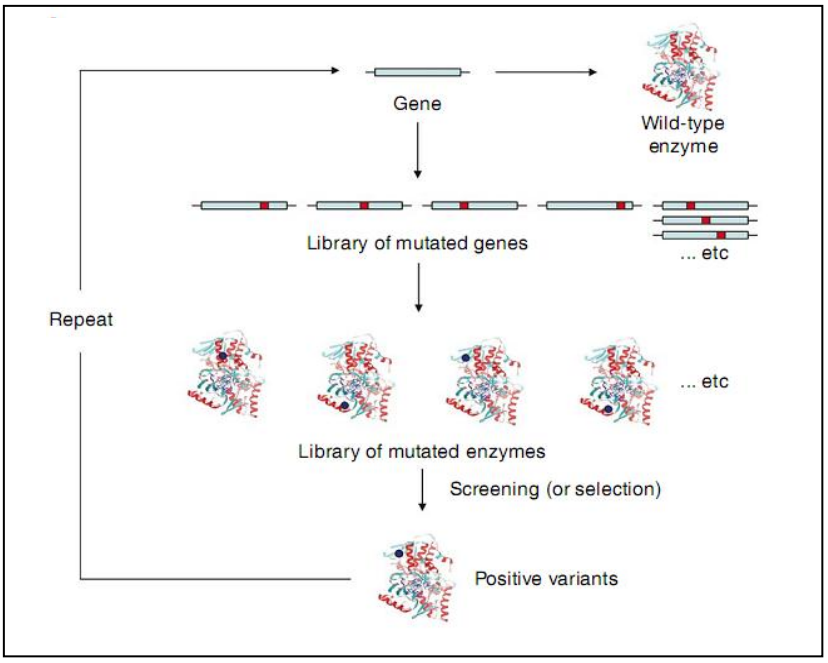

Figure 1.8 The general steps of directed evolution of enzymes. Iterative cycles of random mutagenesis, protein expression and screening or selection of the target activity are performed (Turner, 2009).

Error-prone PCR is a widely used random mutagenesis method; it is a modified PCR reaction with increased frequency of mismatches during DNA synthesis. Another widely used method is DNA shuffling, which is an in vitro gene recombination method. DNA shuffling involves creation of gene fragments by treatment with endonuclease and generation of mutations by random priming of these gene fragments during recombination. This method can be applied to a single gene or a family of homologous genes (Stemmer, 1994, Crameri et al., 1998).

In directed evolution, the availability of a rapid and sensitive assay to identify the improved variants is as important as the achievement of diverse and functional mutant libraries. The crucial steps of screening are physical separation of large cell populations and detection of signal reflecting the enzyme activity. The most frequently used physical separation methods are based on formation of uniform colony development by incubating in growth medium in multi-well plates or by spreading over agar in dishes. The contact between added substrate and the enzyme should develop a signal to enable the monitoring of the enzyme activity. The signal can be formation of color, fluorescence, heat or turbidity (Cohen et al., 2001).

1.4.2.1 Site- Saturation Mutagenesis

Site-saturation mutagenesis is a directed evolution method which lies between random mutagenesis and rational design approaches. It is a more comprehensive study of the structure-based targets or the hot spots identified by random mutagenesis, because it aims to explore all possible substitutions of a chosen residue on the enzyme (Chica et. al., 2005). It may allow understanding of chemical characteristics or sizes of certain positions necessary for structure and/or function of enzymes (Vardar and Wood, 2005a, Buchman et al., 2012).

Site-saturation mutagenesis aims to randomize a targeted position on the protein to any of the other 19 amino acids. Like site-directed mutagenesis, it is an oligonucleotide-based method. However, oligonucleotides are designed so that they carry degenerative codon sequences at the target positions to encode a mixture of mutations at specific positions, rather than a single mutation as in the case of site-directed mutagenesis(Steffens and Williams,2007).

Overlapping-extension PCR can be used for site-saturation mutagenesis (Rui et al., 2005). This method involves two sequential PCR steps. In the first step, two individual extension reactions are performed using (i) a forward primer annealing to 5'-end of the gene and a rear degenerated primer on the mutagenesis site and (ii) a rear primer annealing to 3'-end of the gene and a forward degenerated primer on the corresponding site. The first step results in two gene fragments having an overlapping region on the mutagenesis site. In the second step, these overlapping gene fragments are used in another extension reaction with the forward and the rear to reconstitute the full length gene (Ho et al., 1989) (Figure 1.9).

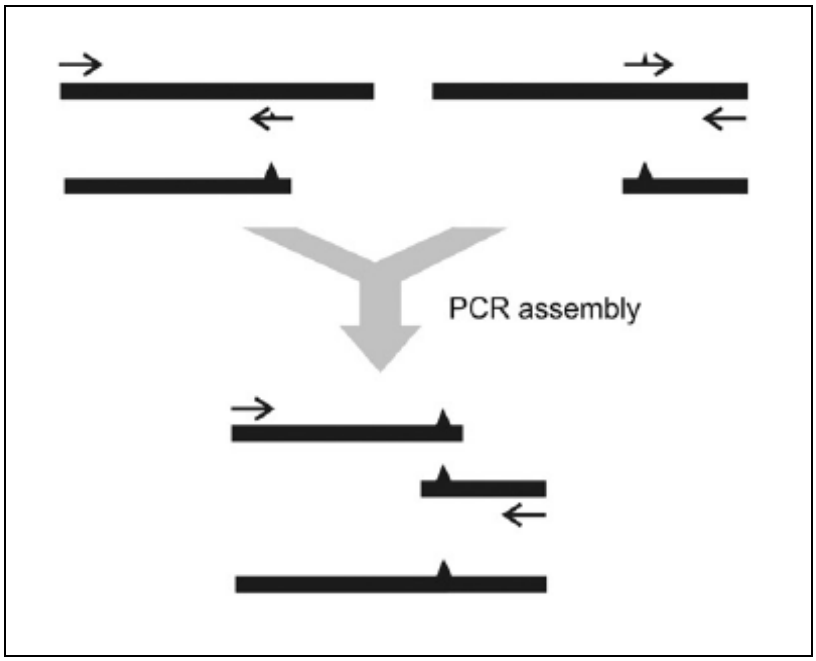

Figure 1.9 The general steps of overlapping PCR. The mutation is introduced into two DNA fragments with a shared sequence at the target site. PCR assembly is performed to regenerate the full length gene (Siloto and Weselake, 2012).

1.4.3 Protein Engineering Studies with ToMO

Toluene monooxygenases perform hydroxylation of a variety of aromatics and have potentials for chemical synthesis and bioremediation of organic pollutants and chlorinated aliphatics as it is emphasized in section 1.3.1. ToMO is highly regiospecific for substrates like phenol, *m*-nitrophenol, and cresols while presenting a relaxed regiopecificity for toluene; it can hydroxylate toluene at *ortho*, *meta* and *para* positions. Both directed evolution and rational design have been applied to understand the control of regiospecific oxidation and catalytic activity of ToMO hydroxylase.

Using DNA shuffling and saturation mutagenesis, Vardar and coworkers discovered that I100, A101, A107, A110, M180 and E214 positions of the alpha-subunit of the hydroxylase are important for catalytic activity (Vardar et al., 2005c, Vardar and Wood, 2005a, Vardar and Wood, 2005b). Later structural studies of ToMO have shown that I100, A107 and M180 occupy the first cavity from the active site. I100 is a gate residue bordering between this cavity and the substrate channel, whereas E214 is located on the surface of the protein forming a gate at the opening of the substrate

channel. I100Q substitution obtained by saturation mutagenesis effected regiospecificity for phenol, catechol, *o*-cresol, *m*-cresol and *m*-nitrophenol and enabled synthesis of novel products hydroquinone, 1, 2, 4-trihydroxybenzene, methylhydroquinone and nitrohydroquinone, respectively (Vardar and Wood, 2004, Vardar and Wood, 2005b). I100Q was also resulted in improved TCE and *cis*-DCE degradation (Vardar and Wood, 2005b). A107T substitution resulted in significant changes in regiospecificity; it was found to be responsible for the conversion of non-specific ToMO into a *para*-acting enzyme (Vardar et al., 2005b). M180 affects the hydroxylation rate and regiospecificity of methyl- and nitro- aromatics. Substitutions of E214 with smaller residues enhanced the oxidation rate of nitroaromatics. For example, variant E214G showed 15-fold increase in *p*-nitrophenol oxidation (Vardar and Wood, 2005a). I100 and E214 were also reported to enhance *cis*-DCE degradation (Vardar and Wood, 2005b).

Based on molecular modeling, it was found that mutations at E103 change the regiospecificity of ToMO (Cafaro et al., 2005). Variants E103G, E103L and E103M were generated by site-directed mutagenesis. The most significant alteration was obtained with variant E103G; it converted ToMO into a *para*-acting enzyme. Also a computational model has been developed for rational design of ToMO mutants for both physiologic and non-physiologic substrates (Notomista et al., 2009, 2011).

CHAPTER 2

MATERIALS & METHODS

2.1 CHEMICALS

All chemicals used in this study are listed in Appendix B.

2.2 BACTERIAL GROWTH and PLASMIDS

Escherichia coli strain TG1, which was used as the host organism of gene cloning and expression, and pBS(Kan)ToMO plasmid, which was used to express ToMO gene cluster, were kindly supplied by Prof. Thomas K. Wood (Penn State University, USA). All bacterial stocks were prepared by adding glycerol (50%, v/v) and stored at -80^{o}C. Luria-Bertani (LB) agar plates containing 100 μg/ml kanamycin were streaked from glycerol stocks and incubated at 37^{o}C for overnight. A single colony was inoculated into 5 ml of LB media containing 100 μg/ml kanamycin and incubated at 37^{o}C with shaking at 250 rpm for 16-18 hours. Plasmid isolation was done by using Nucleospin Plasmid (MACHEREY-NAGEL, Germany) kit according to the manufacturer's manual.

2.3 MUTANT LIBRARY GENERATION

2.3.1 Saturation Mutagenesis by Overlap-Extension PCR

Saturation mutagenesis at selected positions was achieved by overlap-extension PCR. This method includes two steps: (1) Mutations are inserted to gene during

generation of overlapping DNA fragments and (2) Mutated DNA fragments are re-assemble to obtained full-length gene for the cloning.

2.3.1.1 Generating Overlapping DNA fragments

Initial PCRs were prepared to obtain two fragments of *touA* gene which have overlapping ends at target sites by using one set of external primers, which are at the flanking region, and one set of degenerate primers, which carry mutations at the target sites. Table 2.1 lists the primers used in the amplification reactions.

For randomization of position F176 of TouA (499 aa) to other 19 amino acids, F176- Rear and F176- Front primers, which carry NNN at the position encoding F176, were used and ToMO-KpnI-Front and ToMO-SalI-Rear primers, which carry *Mlu*I and *Sal*I restriction sites at the upstream and downstream, respectively. A 700 bp DNA fragment was amplified by using F176-rear and ToMO-*Kpn*I-Front primers and a 957 bp fragment was amplified by using F176-front and ToMO-SalI-Rear primers.

In a similar way, for saturation mutagenesis of F196 of TouA, a 763 bp fragment was amplified by using F196-rear and ToMO-*Kpn*I-Front primers and an 898 bp fragment was amplified by using F196-front and ToMO-*Sal*I-Rear primers.

For saturation mutagenesis of Q204 of TouA, a 782 bp fragment was amplified by using Q204-rear and ToMO-*Kpn*I-Front primers and an 875 bp fragment was amplified by using Q204-front and ToMO-*Sal*I-Rear primers.

Amplification of DNA fragments was achieved in two separate reaction tubes by adding 50 ng of pBS(Kan)ToMO, 30 pmole of appropriate primers 1 mM of $MgCl_2$, 200 µM of dNTPs, 1X *Pfu* Ultra II reaction buffer and 2.5 U, *Pfu* Ultra II DNA polymerase. The reaction mixtures were subjected to initial denaturation (2 min, 96ºC), then 30 cycles of denaturation (45 sec, 96ºC), annealing (45 sec, 55ºC) and extension (2.5 min, 72ºC) and incubated for final extension (10 min, 72ºC) by using a thermal cycler (VWR, Gene Technologies, UK). The PCR products were analyzed on a 1% agarose gel containing 1x TAE buffer and ethidium bromide (0.5 µg/ml). PCR product purification step was done by using Nucleospin Extract II (MACHEREY-NAGEL, Germany) clean-up kit.

2.3.1.2 Assembly PCR

Overlapping DNA fragments from initial set of reactions were used in a subsequent assembly PCR to reconstruct the full length gene. For all three libraries, an assembly PCR mixture was prepared by adding at least 200 ng of purified overlapping DNA fragments (1:1 molar ratio), 30 pmole of ToMO-*Kpn*I-Front and ToMO-*Sal*I-Rear primers, 1 mM of $MgCl_2$, 200 μM of dNTPs, 1X *Pfu* Ultra II reaction buffer and 2.5U, *Pfu* Ultra II DNA polymerase. PCR reaction conditions were same as previous. All volume of PCR mixture was loaded into a 0.7 % agarose gel containing 1x TAE buffer and ethidium bromide (0.5 μg/ml). 1657 bp fragment was cut out from the gel and purified by using Nucleospin Extract II kit to ensure that only full-length *touA* fragment was isolated.

Table 2.1 Primers used in saturation mutagenesis.

Primer	Sequence
ToMO-SalI-rear	5’-CCCACTCATAATCATGAGCGTCG-3’
ToMO-KpnI-front	5’-CCGGCTCGTATGTTGTGTGGAATTGTGAGCGG-3’
F176- rear	5'-GGTCATCATCATGTCGTCNNNGAAAGACCGTGCAGCGATTG-3'
F176- front	5'-CAATCGCTGCACGGTCTTTCNNNGACGACATGATGATGACC-3'
F196-rear	5'-GCATATTGGTGAAGCCTGTTTCNNNTGCGAAGGTCAGCATGATAGAG-3'
F196-front	5'-CTCTATCATGCTGACCTTCGCANNNGAAACAGGCTTCACCAATATGC-3'
Q204-rear	5'-GCGGCCAAACCGAGAAANNNCATATTGGTGAAGCCTGTTTCG-3'
Q204-front	5'-CGAAACAGGCTTCACCAATATGNNNTTTCTCGGTTTGGCCGC-3'

2.3.2 Restriction Enzyme Digestion

pBS(Kan)ToMO and the assembly PCR products were cleaved with *Sal*I and *Mlu*I restriction enzymes (NEB, UK) simultaneously. Reaction mixture contained 1.5 mg of DNA, Bovine Serum Albumin (10μg/ml), NEBuffer 3 and dH_2O and incubated at 37^oC for 4 hours and enzymes were inactivated at 65^oC for 20 min. All volume of

digestion mixtures were loaded into a 0.7 % agarose gel containing 1x TAE buffer and ethidium bromide (0.5 μg/ml). Vector DNA fragment (7669 bp) and insert DNA fragment (1314 bp) were cut out from gel and purified by using Nucleospin Extract II kit.

2.3.3 DNA Ligation

After the double enzyme digestion, the vector and the insert DNA fragments carried sticky ends which were complementary to each other. Ligation reaction was prepared as molar ratio of insert to vector to be 3:1. Ligation reaction mixture contained at least 500 ng of total DNA of vector and insert, T4 ligase (Fermentas, USA) and 1x T4 ligase buffer. Vector amount needed to be used per 100 ng of insert DNA was calculated according to formula given in equation 1.1 below.

$$\text{Vector (ng)} = 100 \text{ ng} \times (1/3) \times [\text{vector size (bp)}/ \text{ insert size (bp)}] \quad (1.1)$$

Ligation mixture was incubated at 16 ^{o}C for overnight and enzyme inactivated at 65ºC for 20 min. Ligation product was cleaned by butanol precipitation; 10 volume of butanol added for 1 volume of reaction mixture and spinned at maximum speed in a bench-top centrifuge for 10 min. Liquid phase was discarded and pellet was vacuum dried until all butanol evaporated and 10μl dH_2O was pipetted onto pellet and kept on ice to allow it dissolve.

2.3.4 Transformation

2.3.4.1 Competent Cell Preparation

Competent cells were always prepared freshly on the same day of transformation. 20 ml of LB media was inoculated by adding 3-5 single colonies from overnight grown *E. coli* strain TG1 on LB-agar plates. Culture was grown until reaching to 0.55-0.60 OD at 600nm. All steps were performed on ice. Cells were harvested at 6000 rpm, at 4^{o}C for 10 min and washed with 1 volume of ice-cold sucrose (300 mM) and harvested again. Cells were washed with ½ volume of sucrose and centrifuged at 6000 rpm, 4^{o}C for 1 min and supernatant was discarded completely. Finally, cell pellet was resuspended in 1/200 volume of sucrose and used immediately.

2.3.4.2 Electroporation

40 µl of freshly prepared competent cells were transferred into ice-cold electroporation cuvettes and 10 µl of ligation mixture was pipetted onto it gently. After applying one pulse (25 µF; 200 Ohm; 1.5 kV on a Bio-Rad GenePulserXcell™), 1 ml of LB medium was added at once, and the cells were transferred to a sterile 1.5ml tube and shaken for 1 h at 37°C. 100 µl of cell mixture was spreaded on each LB-kanamycin (100µg/ml) plate and incubated at 37°C overnight.

2.3.5 Library Master Plates

Master plates were prepared by transferring single colonies onto fresh LB-Kanamycin (100µg/ml) plates from the original transformation plates. Each master plate was prepared to contain 25-50lcolony streaks and was labeled systematically. Master plates were incubated overnight at 37°C and kept 4°C until the screening completed.

2.4 MUTANT LIBRARY SCREENING

2.4.1 Agar-Plate Assay

Mutant libraries were first streaked onto LB-kanamycin agar plates containing 1% glucose (w/v) to suppress the expression of ToMO from *tou* operon. Glucose plates were labeled as same on their respective master plate. Each plate contained three wild-type (*E .coli* TG1/ pBS(Kan)ToMO) streaks as positive controls. Plates were inoculated at 37^{o}C for overnight. Colonies were lifted with the aid of a nylon membrane and placed onto fresh LB-kanamycin agar plates, supplemented with 1 mM substrate (phenol, *p*-cresol or *o*-cresol). The plates were incubated in an airtight chamber for at least 24 h at room temperature. Color formation around cells was observed and compared to wild-type. Wild type ToMO expressing-cells formed orange color around them due to the formation of catechol derivatives of phenol and *o*-cresol. Cells with dark brown or red halo formation were expected as an indication of other dihydroxy-derivatives of phenol or *o*-cresol. The colony color was another feature compared to the wild-type. ToMO expressing cells had a blue colony color and the color density varies with the activity. A second round of screening was repeated for the selected candidates. And after final

candidate selection, 5 ml of LB-kanamycin media was inoculated by transferring cells from the corresponding streaks on the master plates. The plasmids were isolated and also glycerol stocks (50%) were prepared to store at –80 ^{o}C.

2.4.2 DNA Sequence Analysis

Primers used for DNA sequencing are listed in Table 2.2. DNA sequencing had been done commercially. The sequence data was processed by using Vector NTi Advance 10^{TM} software to identify the mutations.

Table 2.2 Primers used in DNA sequencing of mutants.

Library	Primer	Sequence
F176	Q204N-Front	5'-CGAAACAGGCTTCACCAATATGNNNTTTCTCGGTTTGGCCGC-3'
	Q204N-Rear	5'-GCGGCCAAACCGAGAAANNNCATATTGGTGAAGCCTGTTTCG-3'
F196	F269N-Rear	5'-CCGGTGAGTACCGANNNAAGCTTCCAAGATCGCCAGATTGCG-3'
Q204	F269N-Rear	5'-CCGGTGAGTACCGANNNAAGCTTCCAAGATCGCCAGATTGCG-3'
	D211N-Front	5'-TCTCGGTTTGGCCGCTNNNGCTGCTGAGGCCGG-3'

2.5 WILD-TYPE and MUTANT ToMO CHARACTERIZATIONS

2.5.1 Growth Curve of *E. coli* TG1/pBS(Kan)ToMO

50 ml of LB-kanamycin media was inoculated with 0.5 ml of an overnight grown culture. Absorbance at 600 nm was measured by using a spectrophotometer (Jenway 6300, UK) every 30 min for 5 hours. Optical density was plotted against time (min). It was estimated that a healthy culture was at the late exponential phase when OD_{600} reached 2-2.50.

2.5.2 Total Protein Assay

Total protein content of *E. coli* TG1/pBS(Kan)ToMO at the late exponential phase was determined by using MACHEREY-NAGEL Protein quantification kit (Düren, Germany). Bovine Serum Albumin (BSA) was provided with the kit as a protein standard. The dilutions of BSA were prepared according to the manufacturer's manual. 2 µl of dilution samples was placed onto NanoDrop (Thermo Scientific) and absorbance at 570 nm was measured. Standard BSA curve was derived by plotting protein concentration (mg/ml) against absorbance at 570 nm. For sample preparations, two parallel cultures of 20 ml of *E. coli* TG1/pBS(Kan)ToMO culture harvested at late exponential phase by centrifugation at 6000 rpm for 10 min. Pellet was centrifuged for an additional 2 min to remove all the remaining LB and kept at -20^{o}C till the experiment day. Pellet was dissolved in 1/10 volume (2 ml) of Tris-EDTA buffer (pH 7.8) and absorbance at 600 nm (1:100 dilution) measured twice by using spectrophotometer and their average was calculated. Cell disruption was achieved by sonication for 30 seconds in 10 cycles with 3 minutes waiting in between cycles. Cell debris was removed by centrifugation at 9500 rpm for 20 min at 4^{o}C, and the supernatant phase was used protein assay. The sample preparation was same as the BSA standard preparation. Two parallel assays were done for each sample. The protein amounts of samples were calculated by using the formula obtained from BSA standard curve. Total protein content of TG1 expressing ToMO was found to be 0.11 [mg protein/ml.OD_{600}].

2.5.3 Whole-Cell Enzymatic Biotransformations

E. coli TG1/pBS(Kan)ToMO and mutants were streaked onto LB-kanamycin agar plates from their glycerol stocks and incubated overnight at 37^{o}C. 5 ml of LB-kanamycin media was inoculated by transferring a single colony from plates and grown with shaking at 37 ^{o}C for 16-18 hours. 1/100 dilutions of overnight cultures were inoculated into LB-kanamycin media in Erlenmeyer flasks. Cells were harvested at late exponential phase by centrifugation at 6500 rpm for 5 min at room temperature. Pellets were washed with 1 volume of 50 mM Tris-HNO_3 buffer (pH 7-7.3) and centrifuged again. Pellets were resuspended in 1/10 volume of 50 mM Tris-HNO_3 buffer and absorbance of cell suspension at 600 nm was recorded. Cell suspensions were transferred into 10 ml glass vials. Each vial contained 1.5 ml of cell suspension for phenol and naphthalene oxidation and 1 ml of cell suspension for toluene oxidation.

Substrates were added onto cells from ethanol stock solution of phenol and toluene and from DMF stock solution of naphthalene, as final concentration of substrates to be 0.8 mM for phenol, 5 mM for naphthalene, 0.25 mM for toluene. Each vial was capped with a Teflon-coated septum and aluminum seal. The vials were shaken at 250 rpm (New Brunswick Scientific, USA) at 25^{o}C from 5 min to 2 hours of contacting time (depending on the substrate). The vials were collected periodically and frozen to stop the reaction. Samples were thawed on ice and transferred in to 1.5 ml reaction tubes and centrifuged at 13000 g in a bench-top centrifuge for 3 min twice. The supernatants were transferred into HPLC vials. For toluene hydroxylation samples, thawed cells were mixed with an equal volume of methanol (20%) solution before the centrifugation step.

2.5.4 Analytical Methods

2.5.4.1 Toluene Hydroxylation

Astec Cyclobond I2000 Column (SupelCo Analytical, USA) was used for the analysis of toluene hydroxylation. The isocratic elution was performed with milli-Q H_2O and methanol as the mobile phase (80:20) at a flow rate of 1 ml/min. Chemicals were identified by comparing retention times and UV–visible spectra to those of the *o-, m-, p-* cresol and toluene standards.

2.5.4.2 Phenol Hydroxylation

Inertsil C8-3 Column (GL Sciences Inc., Japan) was used for the analysis of phenol hydroxylation. The isocratic elution was performed with acidic H_2O (0.1% formic acid) and acetonitrile as the mobile phase (90:10) at a flow rate of 1 ml/min. Chemicals were identified by comparing retention times and UV–visible spectra to those of the catechol, resorcinol, hydroquinone and phenol standards.

2.5.4.3 Naphthalene Hydroxylation

Inertsil C8-3 Column (GL Sciences Inc., Japan) was used for the analysis of naphthalene hydroxylation. The isocratic elution was performed with acidic H_2O (0.1% formic acid) and acetonitrile as the mobile phase (70:30) at a flow rate of 1 ml/min. Chemicals were identified by comparing retention times and UV–visible spectra to those of the 1-naphthol, 2-naphthol and naphthalene standards.

2.5.5 Sodium Dodecyl Sulfate (SDS)-Polyacrylamide Gel Electrophoresis

The relative protein expression from *touA* loci by *E. coli* TG1/pBS(Kan)ToMO, *E. coli* TG1/pBS(Kan)ToMO-F176H and *E. coli* TG1/pBS(Kan) (negative control) were analyzed using sodium dodecyl sulfate (SDS)-polyacrylamide gel electrophoresis with 12 % acrylamide separating gel and 8 % stacking gel containing 1 % SDS (Table 2.3). Cells were harvested at the late exponential phase and pellets were washed with 1 volume of Tris-EDTA buffer (pH 7.8) and centrifuged at 6000 rpm for 10 min at 4°C. Cell pellets were resuspended in 0.02x volume of Tris-EDTA buffer. Cell suspensions were mixed with loading buffer (tris–glycine buffer containing 2% SDS, 0.1 % bromophenol blue and 100 mM dithiothreitol) and incubated in boiling water for 10 min. Electrophoresis were carried out in Tris–Glycine running buffer containing 0.1% SDS at a constant voltage of 150V for 1 hour (during stacking gel) and 180V for 5 hours (separating gel). Gels were stained with 0.025 % Coomassie Brilliant Blue R-250 solution for 1 hour at shaking and were destained in 10% acetic acid solution for overnight min at room temperature.

Table 2.3 Reagent used for preparation of SDS-polyacrylamide gel.

Reagent	**12% Resolving**

		5% Stacking
ddH_2O	13.2 ml	6.8 ml
30% Acrylamid/Bis	16.0 ml	1.7 ml
Tris Buffer	10 ml (1.5 M Tris-HCl, pH 8.8)	1.25 ml (1.0 M Tris-HCl, pH 6.8)
10% SDS	0.4 ml	0.1 ml
10% APS	0.4 ml	0.1 ml
TEMED	16 µl	10 µl
TOTAL	40 ml	10 ml

CHAPTER 3

RESULTS

3.1 MUTANT LIBRARY SCREENING

Saturation mutagenesis at amino acid positions TouA F176, F196 and Q204 were performed to study their role in regiospecific oxidation of aromatics. More than 3000 colonies were obtained during the construction of F176 and F196 libraries and Q204 library included around 1300 colonies. Libraries had a mixture of blue (indigo producing) and white colonies (Figure 3.1a-b). It is required to screen at least 292 colonies to cover all the possible mutations with 99% probability (Rui et al., 2004). The mutant libraries were screened on phenol, *p*-nitrophenol or *o*-cresol containing agar plates. 870 random colonies (including both blue and white colonies) of F176 library and 850 random colonies of F196 library were screened. 2/3 of the screened colonies from Q204 library turned to be inactive; therefore screening was limited to 360 colonies for this library.

E. coli TG1 cells expressing the wild type ToMO formed dark-orange halo around its mass. Cells with dark-brown or red halo-formation were regarded as an indication of production of hydroquinone, resorcinol from phenol or their methyl-derivatives from *o*-cresol and *p*-cresol (Figure 3.1c-d). These were chosen as mutant candidates and screened at least twice and sequenced to identify the amino acid changes. Table 3.1 summarizes the library size and number of screened colonies from each library.

Table 3.1 Summary of library screening.

Library	Size	Screened	Rescreened	Number of different mutants	Screening substrate
F196	> 3000	870	~ 50	7	phenol and *p*-NP
F176	>3000	850	~ 50	4	phenol
Q204	~1300	360	~ 50	5	*o*-cresol

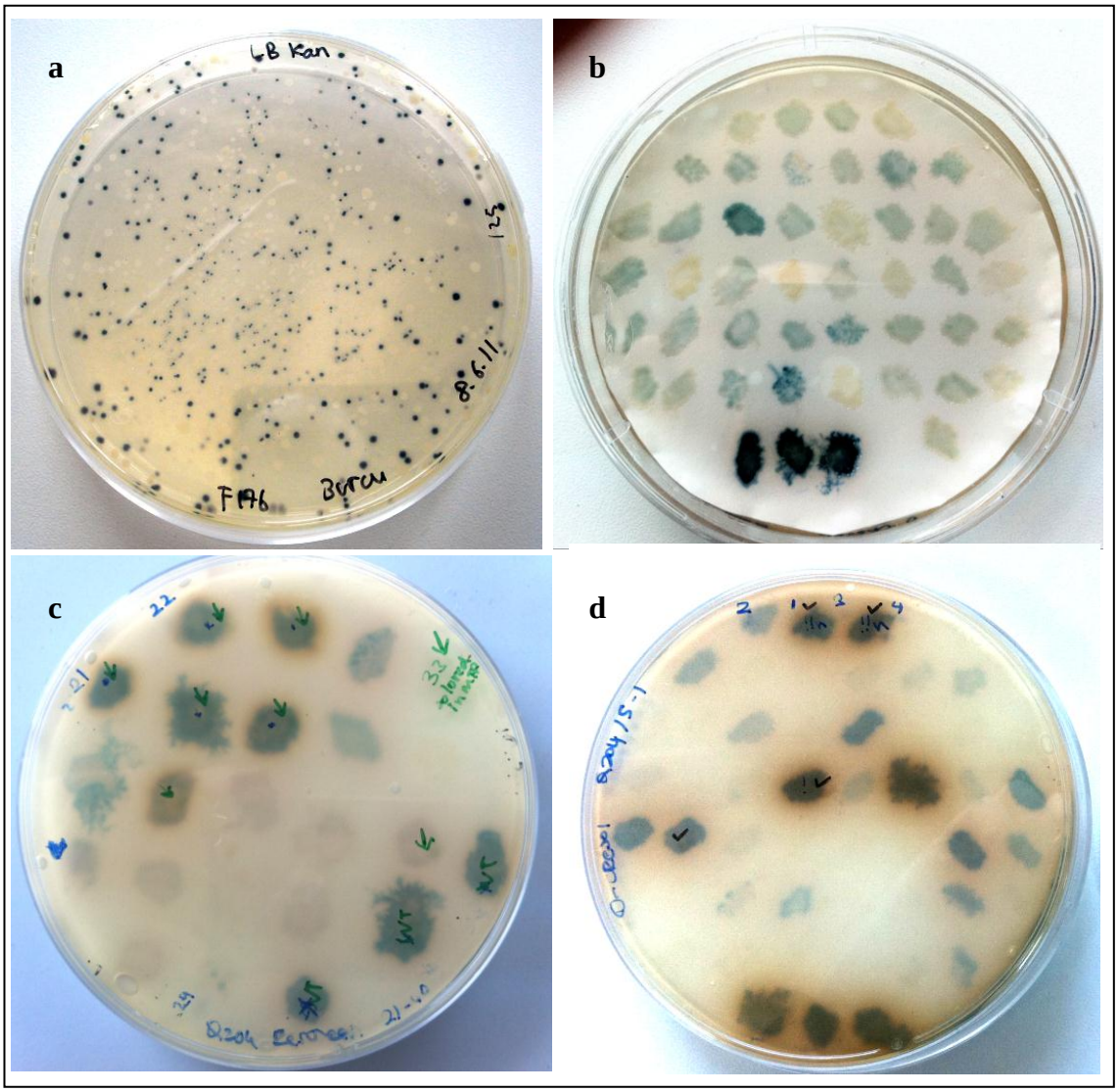

Figure 3.1 Examples of mutant libraries and screening plates: (a) mutant library, (b) indigo formation and (c-d) halo-formation on screening plates containing *o*-cresol.

DNA sequence analysis of the selected candidates revealed that 7 different amino acid substitutions were obtained among 17 mutants of F196 library; 4 different substitutions were obtained among 11 mutants of F176 library and 5 different substitutions of Q204 position among 9 mutants. Two mutants from Q204 library carried an additional mutation. Table 3.2 summarizes the mutants generated in this study.

Table 3.2 List of mutants obtained by site-saturation mutagenesis of TouA F176, F196 and Q204 positions.

Library	Substitution	Mutation	Occurrence
F196	Alanine	GCC	1
		GCT	1
	Valine	GTG	1
	Leucine	CTC	1
		CTA	2
		TTG	2
	Isolucine	ATC	1
	Tyrosine	TAT	3
		TAC	1
	Theroine	ACA	2
		ACT	1
	Histidine	CAT	1
F176	Serine	AGT	1
	Theroine	ACG	1
		ACT	1
		ACA	2
	Asparagine	AAT	1
	Histidine	CAC	3
		CAT	2
Q204	Alanine	GCT	2
	Histidine	CAT	1
		CAC	1
	Theroine	ACC	1
	Serine	TCA	1
	Glutamate	GAA	1

3.2 CHARACTERIZATION OF MUTANTS and WILD-TYPE TOMO

3.2.1 Growth Curve of Recombinant *E .coli* TG1

E. coli TG1 was used as host organism for recombinant expression of ToMO and its variants. Growth of *E. coli* TG1/pBS(Kan)ToMO was monitored over 5 hours of incubation at 37^{o}C. Optical density of cell samples were measured at 600 nm in 30 min intervals.

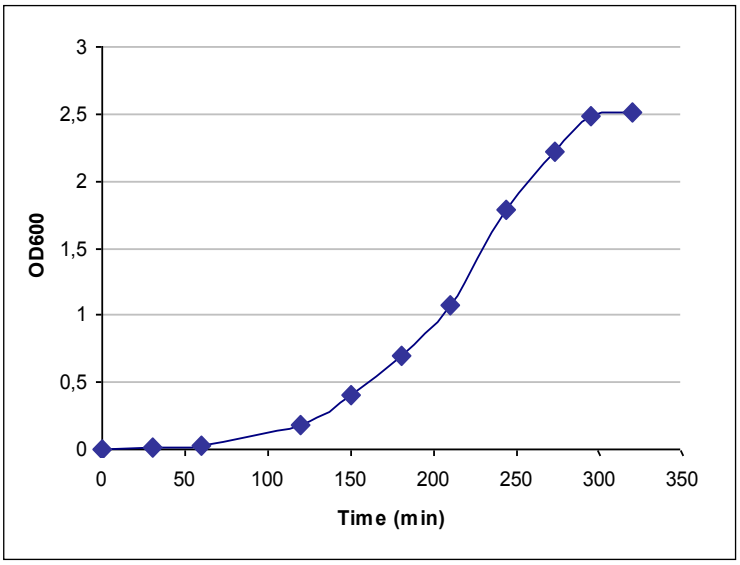

Figure 3.2 Growth curve of *E. coli* TG1/pBS(Kan)ToMO.

Lag phase of *E. coli* TG1 harboring pBS(Kan)ToMO plasmid was found to be around 1 hour. The exponential (log) phase, at which cell doubling occurs, takes place for approximately 3.5 hours. After this point cells are at stationary phase. All following experiments were performed with cells collected at the late exponential phase, which corresponds to an OD_{600} of 2-2.5 according to measurements with Jenway 6300 spectrophotometer instrument (Figure 3.2).

3.2.2 Total Protein Assay for Recombinant *E .coli* TG1

The protein content of *E. coli* TG1 expressing wild-type ToMO was determined by using Protein Quantification kit (MACHEREY-NAGEL Düren, Germany). This experiment was performed with two parallel cultures (Table 3.3). OD_{600} of cultures used in assay were 0.20 and 0.23 as measured 1:100 dilution. Their absorbance at 570nm was 0.26 and 0.27, respectively. These values correspond to 2.32 mg/ml and 2.41 mg/ml protein according to the formula derived from standard BSA curve, respectively (Figure 3.3). Finally, it was calculated that recombinant *E. coli* TG1 contained 0.11 mg protein/ ml per 1 OD_{600}. This value was used in further initial rate calculations during characterization of the wild-type and the mutants.

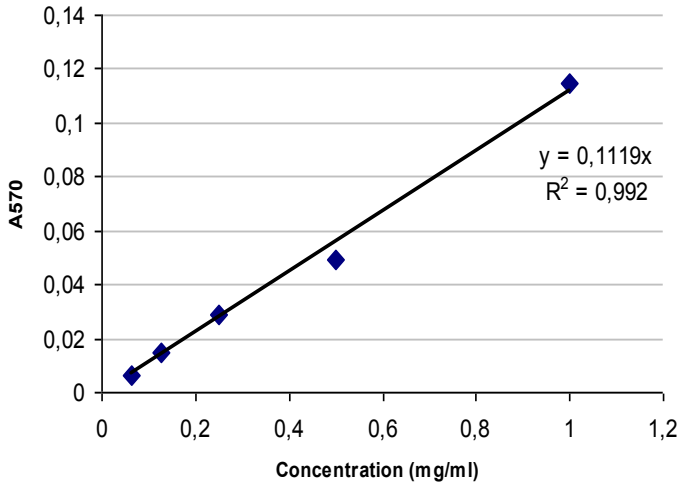

Standard BSA (mg/ml)	A_{570}
0.063	0.0065
0.125	0.0150
0.250	0.0290
0.500	0.0490
1.000	0.1150

Figure 3.3 Standard BSA curve obtained by using cell extract of *E. coli* TG1/pBS(Kan)ToMO.

Table 3.3 Protein assay results of replicate cultures of *E. coli* TG1/ pBS(Kan)ToMO.

Sample	OD (1:100)	A_{570}	Concentration (mg/ml)	Protein content (mg/ml OD)
Culture 1	0.20	0.26	2.32	0.11
Culture 2	0.23	0.27	2.41	0.11

3.2.3 Regiospecificity and Initial Reaction Rates

Wild-type ToMO and mutants were examined for product distribution and initial formation rates by high-performance liquid chromatography (HPLC). Products were identified by comparison with the retention times and UV-visible spectra of standards of commercially available chemicals (Table 3.4). Product peak areas were converted to concentrations by referring to the corresponding standard curves, which were prepared at the maximum absorbance wavelength of each compound (Appendix A). Initial formation rates were determined by using at least three data points of time-course experiments. The regiospecificity of each individual mutant were calculated in terms of the molar product percentages.

Table 3.4 Retention times (RT) and maximum wavelengths (λ_{max}) of standard compounds.

Compound	RT (min)	λ_{max} (nm)
Hydroquinone	5.5	290
Resorcinol	8.7	275
Catechol	11.8	275
o-cresol	4.9	270
m-cresol	5.6	270
p-cresol	7.7	277
1-Naphthol	3.5	324 / 274
2-Naphthol	4.1	324 / 294

3.2.3.1 Wild-Type ToMO

E. coli TG1 cells expressing wild-type ToMO was contacted with toluene. As it was previously reported, ToMO has a relaxed regiospecificity for toluene to produce all three possible products (Vardar and Wood, 2004); ToMO oxidizes toluene at C-2, C-3 and C-4 to produce *o*-cresol (30%), *m*-cresol (19%) and *p*-cresol (51%), respectively (Figure 3.4). Total product formation rate was found to be 0.89 nmol/(min.mg protein) for toluene at 0.25 mM, which is 91µM according to Henry's law (Table 3.5).

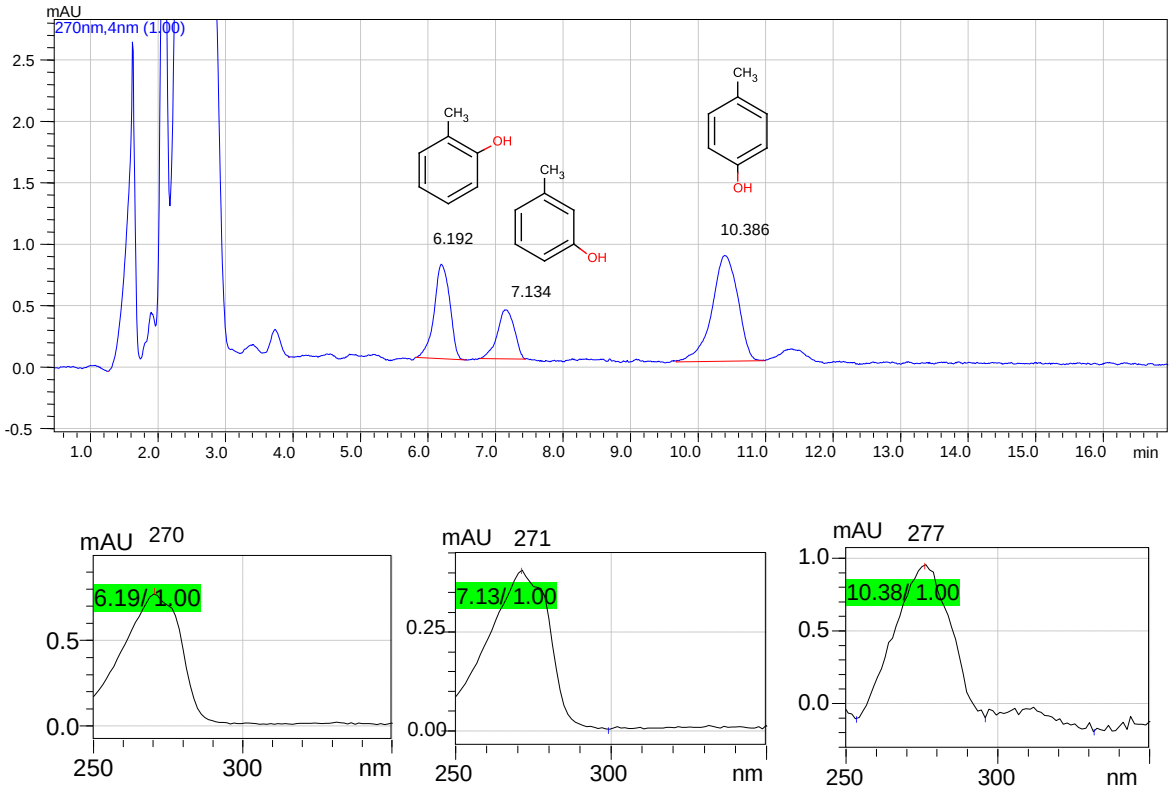

Figure 3.4 HPLC chromatogram of *o*-, *m*-, and *p*-cresols produced from toluene by *E. coli* TG1 expressing wild-type ToMO. Maximum absorption wavelenghts of products are shown at the bottom.

E. coli TG1 expressing wild-type ToMO hydroxylates phenol at C-2 to produce catechol (Vardar and Wood, 2004). Accordingly, catechol was the only product identified from the oxidation of phenol (Figure 3.5). Initial product formation rate from phenol (0.8 mM) was found to be 1.17 nmol/(min.mg protein).

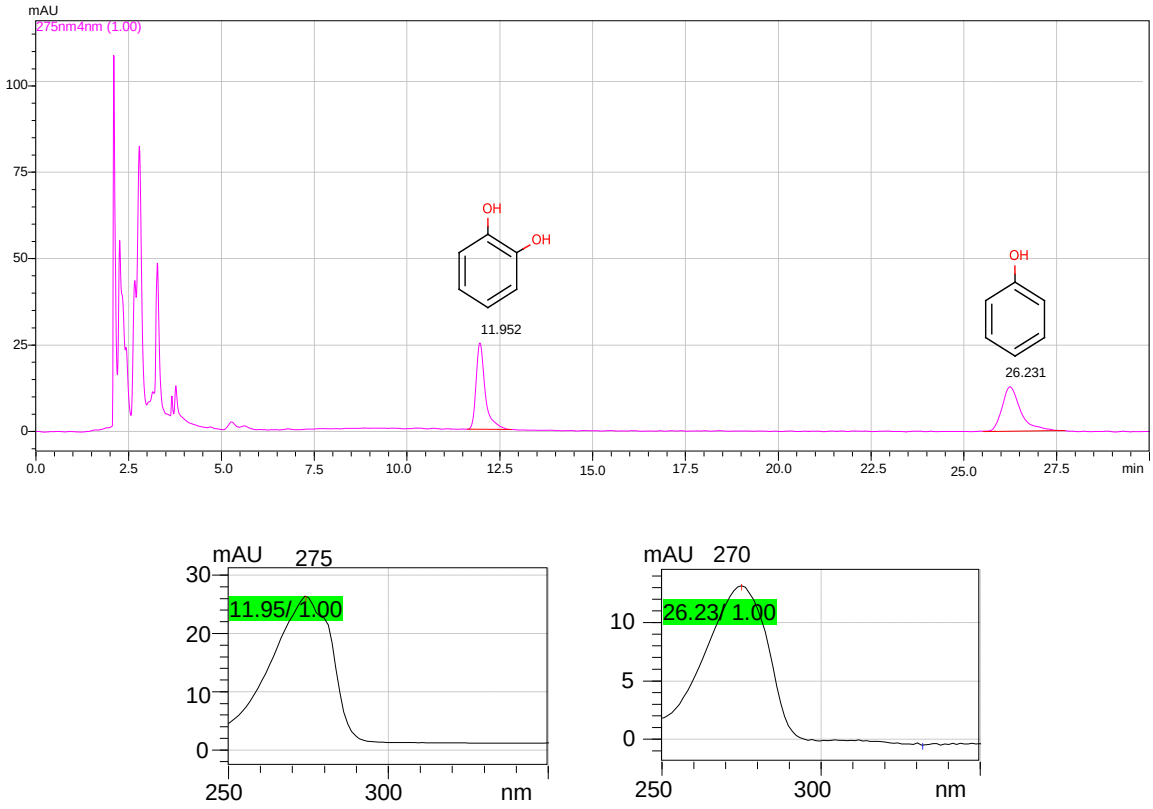

Figure 3.5 HPLC chromatogram of catechol produced from phenol by *E. coli* TG1 expressing wild-type ToMO. Maximum absorption wavelenghts of products are shown at the bottom.

Wild-type ToMO expressing *E. coli* TG1 oxidizes napthalene at C-1 and C-2 to produce 1-naphthol and 2-napthol, respectively (Vardar and Wood, 2005b). Accordingly, figure 3.6 shows that both products were identified from oxidation of naphthalene. Wild-type ToMO produced 85% 1-naphthol and 15% 2-naphthol. Initial product formation rate from naphthalene (5 mM) was found to be 0.80 nmol/(min.mg protein).

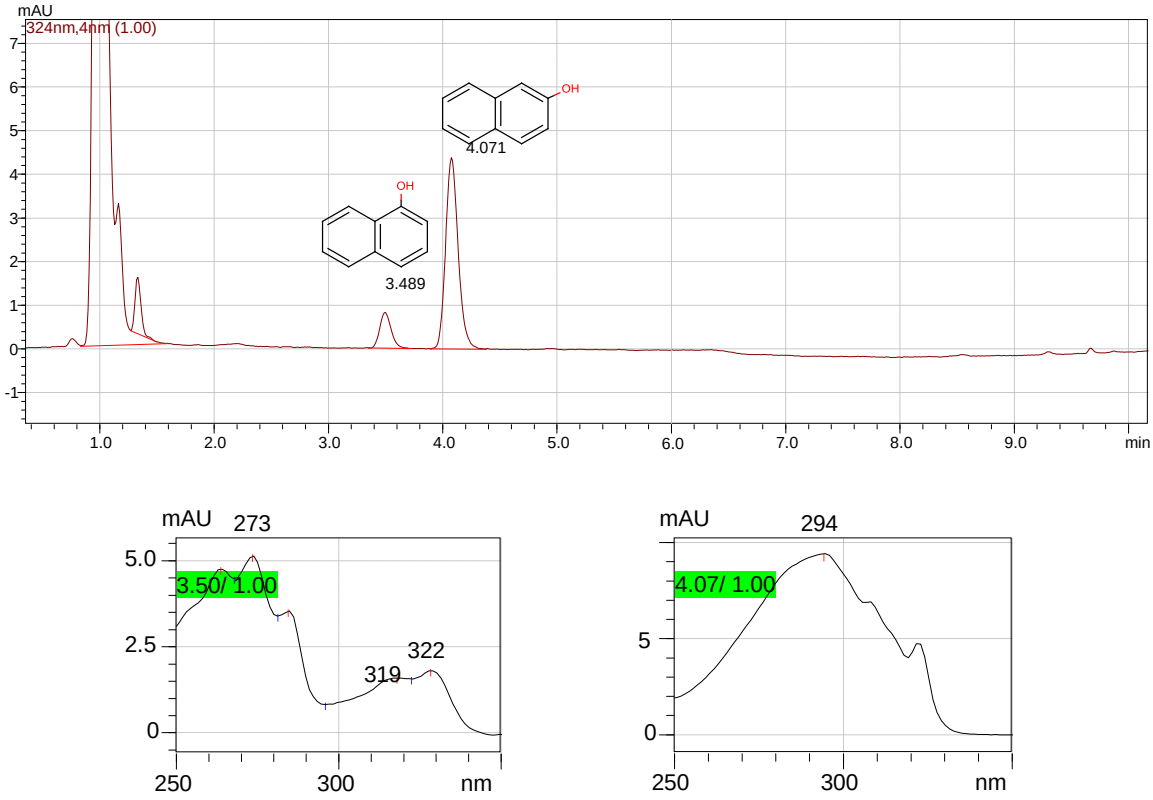

Figure 3.6 HPLC chromatogram of 1- and 2-naphthol produced from naphthalene by *E. coli* TG1 expressing wild-type ToMO. Maximum absorption wavelenghts of products are shown at the bottom.

3.2.3.2 TouA F176 Mutants

TouA F176 variants (F176H, F176N, F176T, and F176S) were characterized for the regiospecific hydroxylation of phenol (0.8 mM), toluene (0.25 mM) and naphthalene (5mM).

Like wild-type ToMO, F176 variants hydroxylated phenol to form catechol, besides different than wild-type ToMO, they have capability of hydroxylation at C-4 to form hydroquinone in varying percentages (Figure 3.11). That is, TouA F176H mutant formed 49% catechol and 61% hydroquinone; TouA F176N formed 23% catechol and 77% hydroquinone; TouA F176S mutant formed 85% catechol and 15% hydroquinone and TouA F176T mutant formed 75% catechol and 25% hydroquinone. HPLC chromatograph of TouA F176H mutant was shown in figure 3.7 to represent the peaks of hydroquinone and catechol of TouA F176 variants.

There were changes in the catalytic rates of TouA F176 variants toward phenol as substrate. TouA F176N, F176S and F176T variants showed around 5.5-, 2.7- and 3.7 fold decreases in total initial formation rates from phenol at 0.8 mM, respectively. On the other hand, F176H variant was found to be an improved with around 5-fold increase in the total initial formation rate under the same conditions.

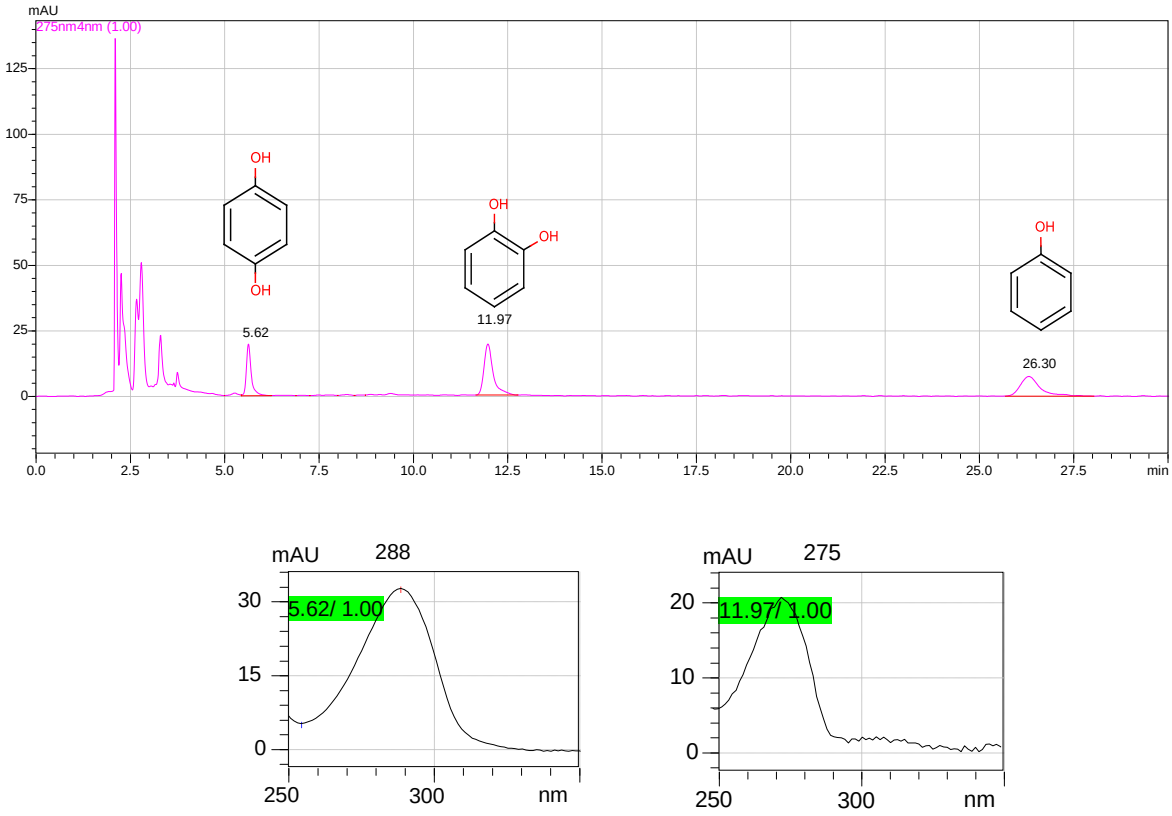

Figure 3.7 Representative HPLC analysis of hydroquinone and catechol produced from phenol by TouA F176H variant. Maximum absorption wavelenghts of products are shown at the bottom.

All variants hydroxylated toluene and formed the three possible regiospecific products like wild-type ToMO did, however the variants showed significant preference for C-4 hydroxylation and yielded more *p*-cresol compared to wild-type (Figure 3.12). That is, TouA F176H mutant formed 12% *o*-cresol, 15% *m*-cresol and 73% *p*-cresol; TouA F176N mutant formed 3% *o*-cresol, 5% *m*-cresol and 92% *p*-cresol; TouA F176S mutant formed 4% *o*-cresol, 7% *m*-cresol and 89% *p*-cresol; TouA F176T mutant formed 6% *o*-cresol, 10% *m*-cresol and 84% *p*-cresol.

The substitutions of TouA F176 also resulted in changes in the catalytic rates of toluene oxidation. TouA F176N variant lost almost half of the activity while TouA F176T variant was as active as the wild-type on 0.25 mM toluene. And, TouA F176S and F176H variants had a 1.85- and 4-fold increase in the initial rates of formation, respectively. Table 3.5 summarizes all the results of characterization experiments performed with TouA F176 variants. HPLC chromatograph of TouA F176S mutant was shown in figure 3.8 to represent the peaks of *o*-, *m*-, *p*-cresols and catechol of F176 variants.

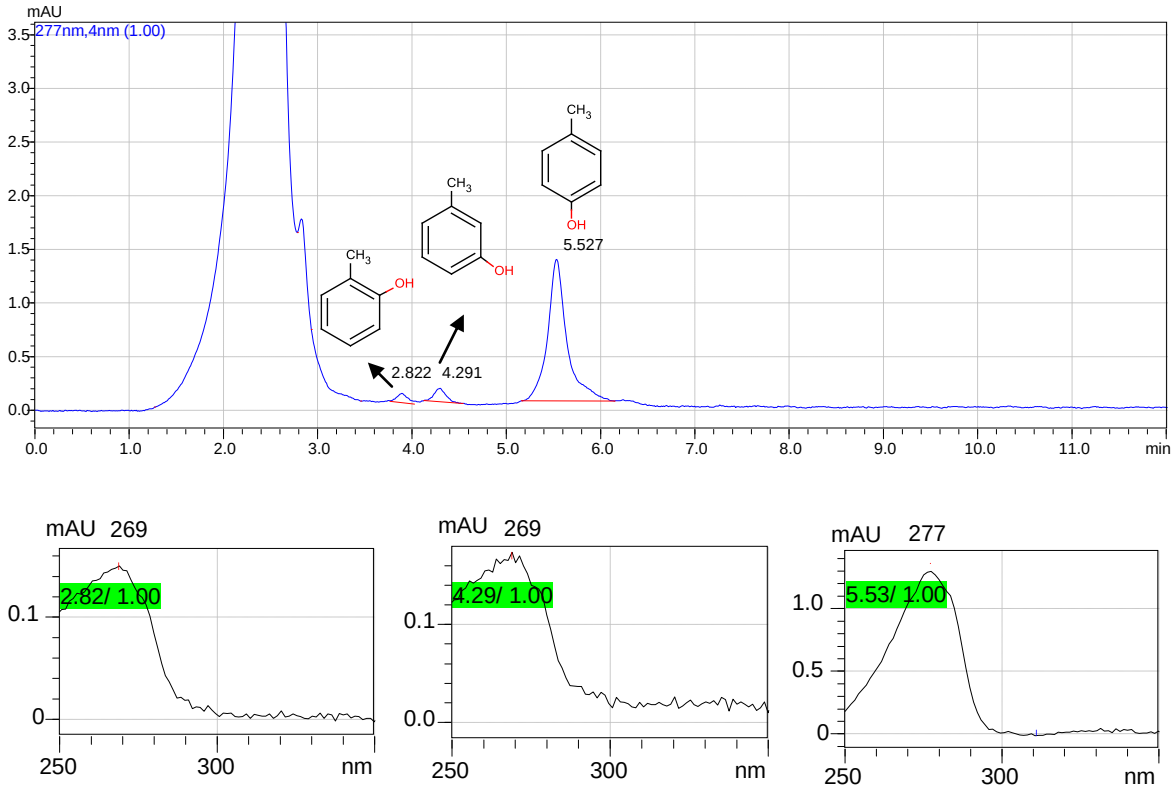

Figure 3.8 Representative HPLC analysis of *o*-, *m*-, and *p*-cresols produced from toluene by TouA F176S variant. Maximum absorption wavelenghts of products are shown at the bottom.

In general, TouA F176 variants showed significant increase in the percentages of 2-naphthol formation from naphthalene oxidation (Figure 3.13). TouA F176H mutant formed 71% 1-naphthol and 29% 2-naphthol; TouA F176N formed 61% 1-naphthol

and 39% 2-naphthol; TouA F176S mutant formed 50% 1-naphthol and 50% 2-naphthol and TouA F176T mutant formed 56% 1-naphthol and 44% 2-naphthol.

The substitutions of TouA F176 also resulted in changes in the catalytic rates toward naphthalene. TouA F176N, F176S and F176T variants showed 1.7-, 3- and 5.7 fold decreases in initial formation rates of naphthols from 5 mM naphthalene, respectively. On the other hand, F176H variant showed around 3-fold increase under the same conditions. The protein expression level of TouA F76H was analyzed by SDS-gel electrophoresis (see *section 3.2.3.3.1*). HPLC chromatograph of TouA F176H mutant was shown in figure 3.9 to represent the peaks of 1- and 2-naphthol of TouA F176 variants.

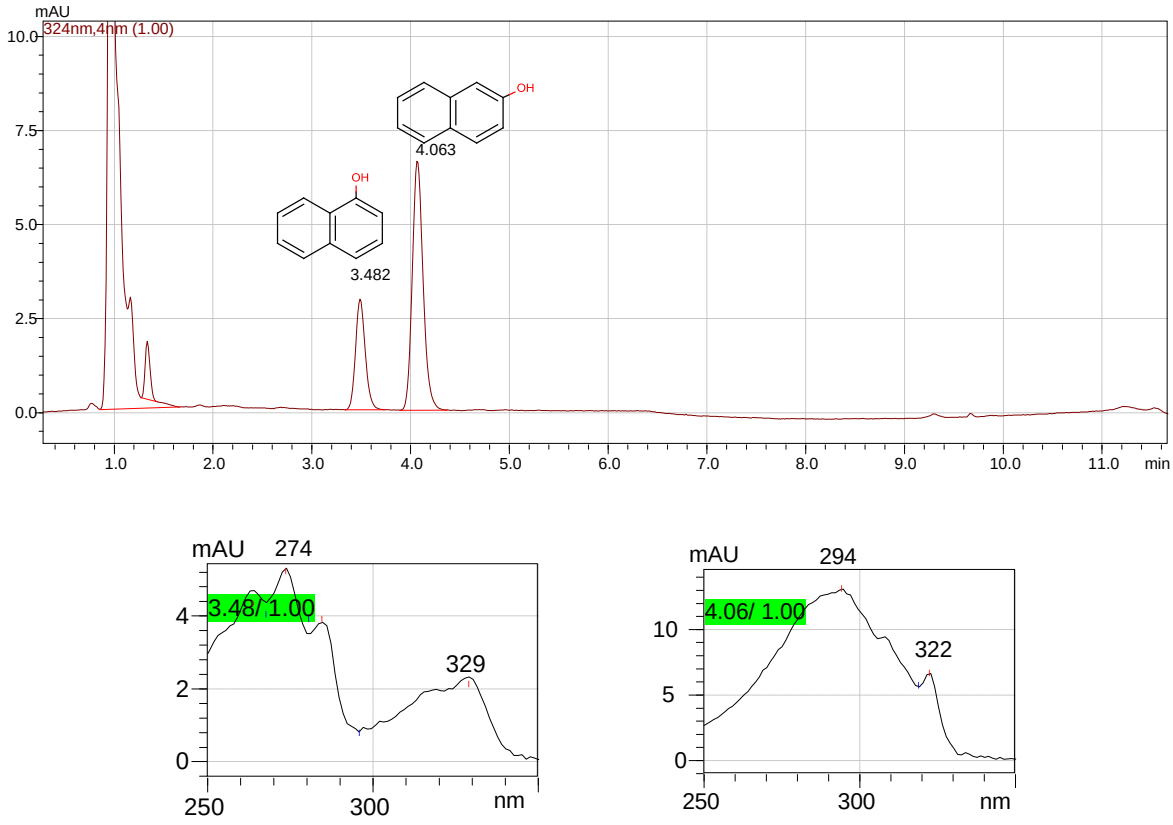

Figure 3.9 Representative HPLC analysis of 1- and 2- naphthol produced from naphthalene by TouA F176H variant. Maximum absorption wavelenghts of products are shown at the bottom.

3.2.3.3.1 SDS-PAGE

The protein expression from *tou* promoter by TouA F176H variant was evaluated by SDS-PAGE. 55 kDa protein band of TouA and 35 kDa protein band of TouE/TouF were observed on the gel (Figure 3.10). The TouA F176H variant showed a similar level of protein expression of TouA subunit compared to that of wild-type ToMO. Hence, the increase in the activity of this variant, which is at least 3-fold for naphthalene oxidation at 5 mM, is due to the single amino acid change rather than the altered expression levels.

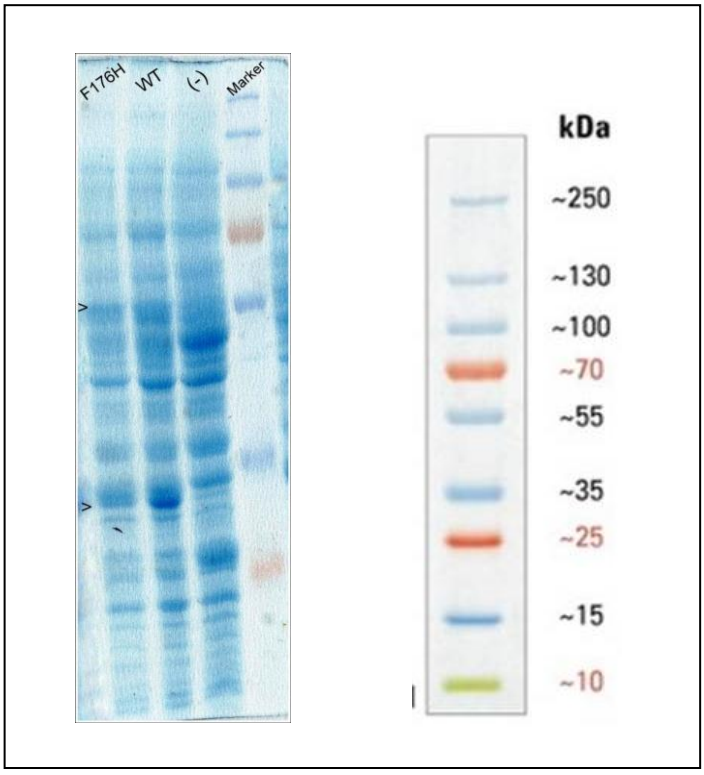

Figure 3.10 SDS-PAGE gel of whole cell proteins of *E. coli* TG1 expressing wild-type ToMO and TouA F176 variant. Negative control was *E. coli* TG1 carrying empty vector, pBS(Kan). 10-250 kDa protein ladder was used as molecular weight standard.

Table 3.5 Initial formation rates and regiospecificity of *E. coli* TG1/pBS(Kan)ToMO expressing wild-type and TouA F176 variants.

Enzyme	Phenol Oxidation (0.8mM)			Naphthalene Oxidation (5mM)			Toluene Oxidation (0.25mM)			
	Regiospecificity (%)		Total Rate (nmol/min.mg protein)	Regiospecificity (%)		Total Rate (nmol/min.mg protein)	Regiospecificity (%)			Total Rate (nmol/min.mg protein)
	Catechol	Hydroquinone		1-Naphthol	2-Naphthol		*o*-Cresol	*m*-Cresol	*p*-Cresol	
Wild-type	100	0	1.17± 0.42	85	15	0.80	30	19	51	0.89± 0.12
F176H	39	61	5.84 ± 1.48	71	29	2.56	12	15	73	3.80 ± 0.90
F176N	23	77	0.21 ± 0.10	61	39	0.47	3	5	92	0.48 ± 0.16
F176S	85	15	0.43 ± 0.10	50	50	0.26	4	7	89	1.64 ± 0.55
F176T	75	25	0.32 ± 0.10	56	44	0.14	6	10	84	0.84 ± 0.17

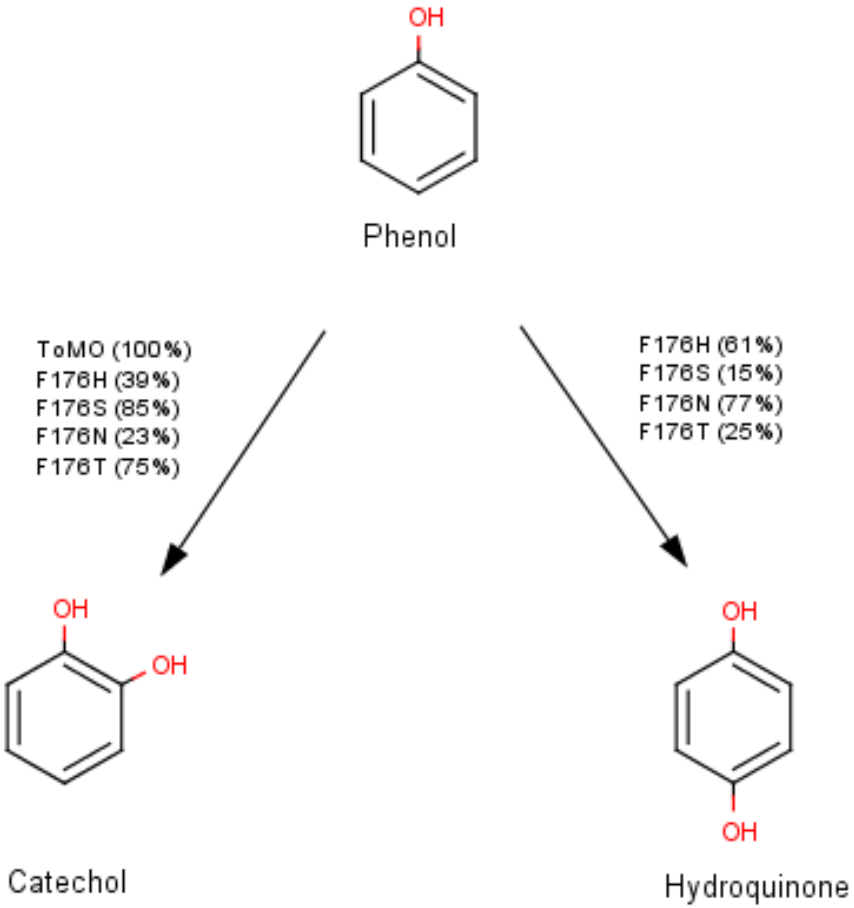

Figure 3.11 Phenol oxidation pathways of wild-type ToMO and regiospecific mutants. Numbers in parenthesis indicate molar product percentages.

3.2.3.3 TouA F196 Mutants

TouA F196 variants were characterized for the regiospecific hydroxylation of phenol, toluene and naphthalene (Table 3.6). All variants hydroxylated phenol and formed catechol like wild-type ToMO. Hydroquinone or resorcinol formations were not detected. There were slight changes in the product distribution for naphthalene and toluene oxidation. TouA F196A showed slight increase in the percentages of 2-naphthol formation from naphthalene, it produced 26% 2-naphthol while wild-type ToMO produced 16% 2-naphthol. And, for toluene hydroxylation, TouA F196I variant had slight decrease in *o*-cresol percentage (14%) and increase in *p*-cresol percentage (70%) in comparison to wild-type ToMO (30% and 51%, respectively) (Figure 3.12).

TouA F196 variants were contacted with phenol at 0.8 mM, naphthalene at 5 mM and toluene at 0.25 mM. Among TouA F196 mutants, F196V substitution resulted in significant decrease in the overall activity for all of the tested substrates. It showed about 3.5-fold decrease in the initial formation rate of catechol from phenol and a 7.5 fold decrease in the initial formation rate of naphthols from naphthalene. While TouA F196T, F196A and F196H retained similar activity to wild-type enzyme for toluene oxidation and phenol oxidation, they had at least 3.5-fold decrease in the initial product formation rate from naphthalene. TouA F176Y and F196L were as active as the wild-type ToMO for phenol oxidation, however both had decreased activity for naphthalene and toluene. TouA F176Y showed about 6.6- and 3-fold decreased initial product formation from naphthalene and toluene, respectively.

Table 3.6 Initial formation rates and regiospecificity of *E. coli* TG1/pBS(Kan)ToMO expressing wild-type and TouA F196 variants.

Enzyme	Phenol Oxidation (0.8mM)		Naphthalene Oxidation (5mM)			Toluene Oxidation (0.25mM)			
	Regiospecificity (%)	Rate (nmol/min. mg protein)	Regiospecificity (%)		Rate (nmol/min. mg protein)	Regiospecificity (%)			Rate (nmol/min. mg protein)
	Catechol		1-Naphthol	2-Naphthol		*o*-Cresol	*m*-Cresol	*p*-Cresol	
Wild-type	100	1.17± 0.42	85	15	0.80	30	19	51	0.89± 0.12
F196A	100	1.07	74	26	0.31	29	25	46	1.18
F196V	100	0.34	84	16	0.04	ND*	ND	ND	ND
F196L	100	1.54	85	15	0.42	24	20	56	0.44 ± 0.18
F196I	100	0.63	79	21	0.13	14	16	70	0.23
F196T	100	1.18	82	18	0.15	24	15	61	0.91
F196Y	100	1.12	84	16	0.12	29	19	52	0.29
F196H	100	0.77	86	14	0.12	30	22	48	0.83

*ND: Not determined

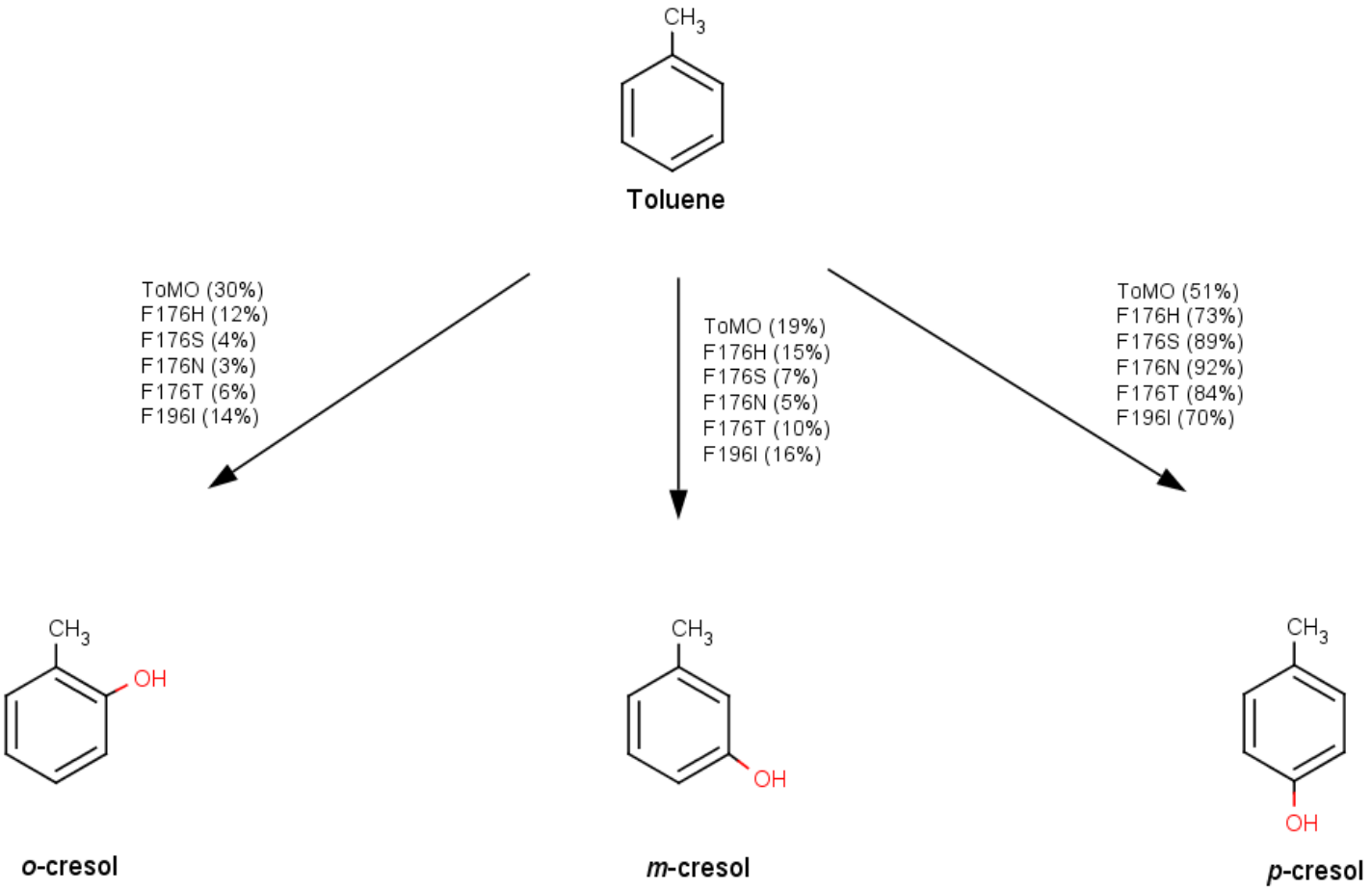

Figure 3.12 Toluene oxidation pathways of wild-type ToMO and regiospecific mutants. Numbers in parenthesis indicate molar product percentages.

3.2.3.4 TouA Q204 Mutants

TouA Q204 variants were characterized for the regiospecific hydroxylation of phenol at 0.8 mM, naphthalene at 5 mM and toluene at 0.25 mM (Table 3.7). All variants formed 100% catechol like wild-type ToMO did. There were slight changes in the product distribution for naphthalene and toluene oxidation. TouA Q204A showed a slight increase in the percentages of 1-naphthol formation; it produced 90% 2-naphthol while wild-type ToMO produced 84% (Figure 3.13).

In general, TouA Q204 variants retained similar or slightly decreased activity for phenol oxidation, except Q204E, which showed about 8-fold decrease of initial formation rate of catechol from phenol. Q204 variants performed significantly lower activity for naphthalene, in particular, Q204T and Q204E lost most of their activities. However, the Q204T variant, and Q204A as well, retained similar activity for toluene compared to the wild-type enzyme.

Table 3.7 Initial formation rates and regiospecificity of *E. coli* TG1/pBS(Kan)ToMO expressing wild-type and TouA Q204 variants.

Enzyme	Phenol Oxidation (0.8mM)		Naphthalene Oxidation (5mM)			Toluene Oxidation (0.25mM)			
	Regiospecificity (%)	Rate (nmol/min.mg protein)	Regiospecificity (%)		Rate (nmol/min.mg protein)	Regiospecificity (%)			Rate (nmol/min.mg protein)
	Catechol		1-Naphthol	2-Naphthol		*o*-Cresol	*m*-Cresol	*p*-Cresol	
Wild-type	100	1.17± 0.42	85	15	0.80	30	19	51	0.89± 0.12
Q204A	100	1.12	90	10	0.11	30	13	57	1.14
Q204T	100	0.88	82	18	0.02	29	16	55	0.78
Q204E	100	0.14	86	14	0.02	35	14	51	0.06
Q204H/A106V	100	0.93	85	15	0.29	38	12	50	0.54
Q204S/S222N	100	ND*	ND	ND	ND	31	12	57	0.06

* ND: Not determined

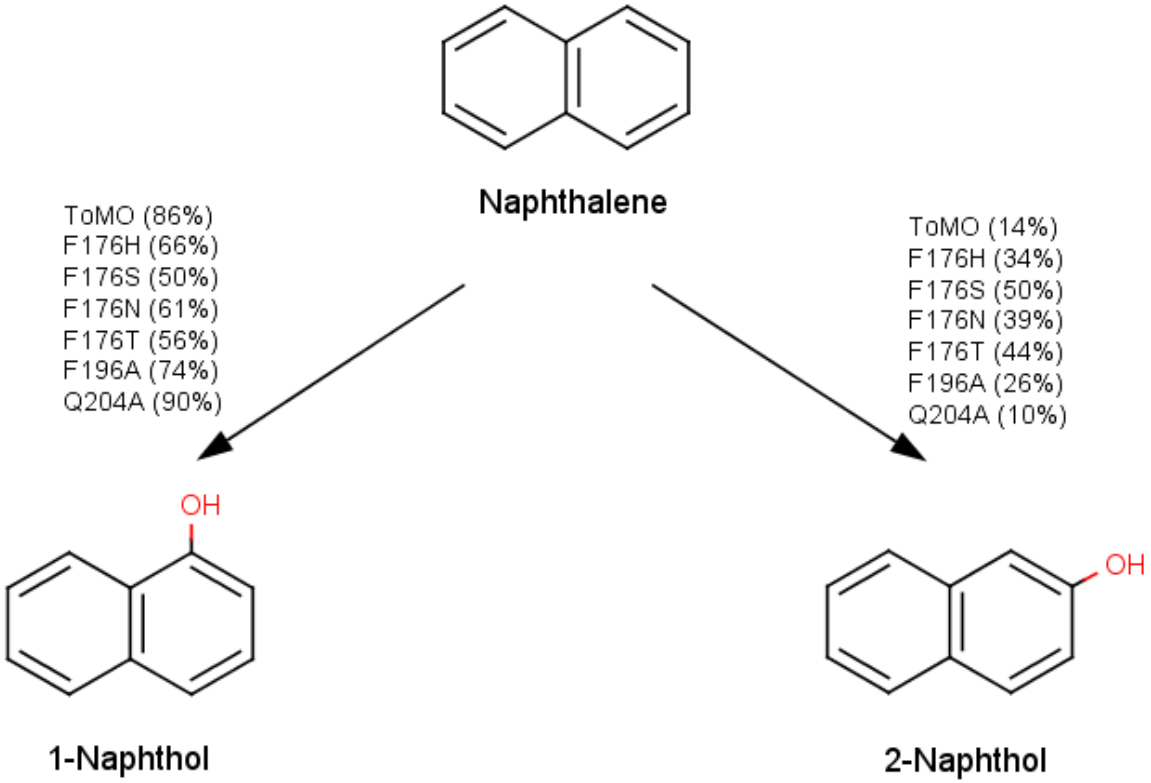

Figure 3.13 Naphthalene oxidation pathways of wild-type ToMO and regiospecific mutants. Numbers in parenthesis indicate molar product percentages.

CHAPTER 4

DISCUSSION

The objective of this project was to investigate the roles of three amino acid positions, TouA F176, F196 and Q204 of toluene/*o*-xylene monooxygenase on the regiospecific oxidation of aromatics.

TouA F176 and F196 are located at the hydrophobic substrate binding cavity which accommodates the diiron center. This cavity is connected to the substrate channel and might be connected to the proposed oxygen route upon conformational changes during catalysis, where I100 may shift its position to control the opening. In the wild-type enzyme, the closest C-C distance of F176 and F196 to I100 is 4.3 and 5.8 Å, respectively (Figure 1.5 and 1.6). Q204 lines the substrate channel and 6.7 Å away from the gate residue, I100 (Figure 1.7)

For studying the selected positions comprehensively, site-saturation mutagenesis was applied to generate libraries of ToMO TouA F176, F196 and Q204 variants. Site-saturation mutagenesis may enable to isolate substitutions which are not predicted by rational design, or site-directed mutagenesis. This approach was used to study the oxidation of toluene and naphthalene by T*p*MO of *Ralstonia pickettii* PKO1 before and TbuA1 G103 and A107 were shown to be important for the regiospecificity (Fishman et al., 2005). Mutant libraries were screened on agar plates for phenol, *o*-cresol and *p*-nitrophenol oxidation based on the colored product formation and also for differences in the colony colors due to indigo formation by ToMO activity. The isolated mutants were characterized for regiospecificity and initial product formation rates of products from phenol at 0.8 mM, toluene at 0.25 mM and naphthalene at 5 mM. The activity assays were performed with whole-cells to achieve expression of the functional enzyme complex and NADH recycling required for the activity. The products of variants were

analyzed by HPLC. DNA sequencing of candidates obtained from library screening revealed that four non-conservative mutations were generated for F176 library, two of which (TouA F176H and F176N) have not been designed by site-directed mutagenesis before.

The results with TouA F176 variants have shown that this position influences the regiospecificity of phenol, naphthalene and toluene oxidation. Even though differences in the percentages, all F176 mutants produced more *para*-substituted products from phenol and toluene and more 2-naphthol from naphthalene compared to wild-type ToMO. These results are in accord with previous studies with TouA F176. Previously, TouA F176I and F176L substitutions were predicted by rational design as a better *para*-acting enzyme for toluene and *o*-xylene and increased percentages of 2-naphthol production from naphthalene. Also, other substitutions of TouA F176 predicted by rational design to prefer *para*-hydroxylation of 2-phenyethanol. Among the F176 variants obtained in this project, TouA F176N was the most regiospecific mutant for hydroquinone formation (77%) from phenol and *p*-cresol formation (92%) from toluene. TouA F176S variant showed the highest shift towards 2-naphthol production (50%) from naphthalene. TouA F176H variant was found to be an "up" mutant for all the tested substrates with at least a 3-fold increase in naphthalene oxidation. This result may suggest that TouA 176, which naturally hydrophobic in nature, can accommodate a hydrophilic and a partially charged amino acid and even have an enhanced activity.

The structure of TouA F176 mutants were built based on X-ray structure of resting state ToMO (PDB: 1T0Q) by using mutagenesis wizard within PyMOL (Figure 4.1). In the mutation module, PyMOL selected the most occurring rotamer for the side chain and kept the rest of the protein unchanged. As a result, the substitution of phenylalanine to histidine at 176 changed the direction of the side chain, and in this configuration the opening of the cavity expands the most among TouA variants. Accordingly, the distance of the closest atom of histidine at 176 to gate residue (I100) was measured 8.1 Å by using PyMOL Software, which is the largest among F176 variants (Table 4.1). In addition, modeling suggests that TouA F176T, F176S and F176N substitutions may adopt side-chain rotamers that may form additional H-bonds with the backbone of A172 and side-chain of E103 on structures of the native ToMO(PDB: 1T0Q) and substrate -bound ToMO (PDB: 1T0S). However, none of

F176H rotamers makes an additional H-bond with its neighbors on both structures (Figure 4.2).

TouA F196 library contained colonies with range of indigo color and, which parallels with the report that T4MO TmoA F196 might be important for the indole oxidation oxidation capability (McClay et al., 2005). By site-saturation mutagenesis, seven substitutions of this position obtained. Among all variants, TouA F196A showed slight increase in percentages of 2-naphthol formation from naphthalene compared to wild-type ToMO (26% and 16%, respectively) and TouA F196I had slight increase in *p*-cresol production from toluene (70%). Overall, this position has no major effect in the product distribution for phenol, toluene and naphthalene oxidation.

TouA F196 substitutions did not cause much impact on the activity of phenol oxidation, except F196V and F196I variants had a significant decrease. For toluene oxidation F196A, F196T and F196H substitutions retained wild-type activity while F196V, F196I and F196Y substitutions resulted in a significant decrease in the activity. And all of the TouA F196 variants were found to be “down” mutants compared to wild-type ToMO for naphthalene oxidation.

The modeling of the mutant side chains at TouA F196 on structure of resting state ToMO (PDB: 1T0Q) suggests that substitutions at this position results in changes in the geometry of the substrate binding cavity (Table 4.1) and also alters the distances of the side chains with respect to iron atoms and gate residue (I100) (Figure 4.2)

Most of the TouA Q204 library lost the indigo production activity and screening of the few active colonies resulted in the isolation of five TouA Q204 substitutions. Two variants carried an additional random mutation. Among tested variants there was no regiospecific alterations for phenol, toluene and naphthalene oxidation, only Q204A had a 5% increase in 1-naphthol formation from naphthalene compared to wild-type ToMO. TouA Q204A and Q204T retained wild-type activity for phenol and toluene oxidation but lost almost 90% of the activity for naphthalene oxidation. TouA Q204E substitution remarkably impaired the capability for oxidation of the tested substrates. The double mutant Q204H/A106V had a decreased activity for naphthalene and toluene while having similar activity to wild-type for phenol oxidation. The other double mutant, Q204S/S222N was originally chosen for its incapability to produce indigo during

mutant screening. The HPLC analysis also showed that this variant lost almost all activity for the tested substrates. However, it is further need to be studied to understand whether the additional mutations were also responsible on the decrease of the activity.

The modeling of the side chains of single mutants of TouA Q204 suggests that these substitutions results in changes in the side change arrangement and the distances to the gate residue and the substrate channel (Table 4.1). In addition, the substitution of polar uncharged glutamine (Q) residue at 204 to a negatively charged glutamate (E) may result in the formation of an H-bonding with side chain of neighboring T273. Also, the substitution to other polar residues, serine and threonine, may generate an additional H-bonding with the backbone oxygen atom of the residue F200.

Table 4.1 Side-chain distances of TouA F176, F196 and Q204 variants with respect to iron atoms, the gate residue I100 and the channel.

	Fe_A (Å)	Fe_B (Å)	I100 (Å)	Channel (Å)
F176	8.8	8.6	4.3	4.3
F176H	9.2	9.0	8.1	7.6
F176N	10.2	9.9	5.8	6.3
F176S	10.7	10.7	6.8	7.1
F176T	10.6	10.4	6.8	7.2
F196	8.0	7.0	5.8	3.5
F196A	10.4	8.4	10.0	7.2
F196I	9.4	7.9	8.4	5.6
F196T	9.6	8.0	8.4	5.7
Q204	10.7	10.7	6.7	3.6
Q204A	11.7	11.7	9.6	6.7
Q204T	12.0	12.4	8.9	5.1
Q204E	11.5	11.6	7.5	3.8

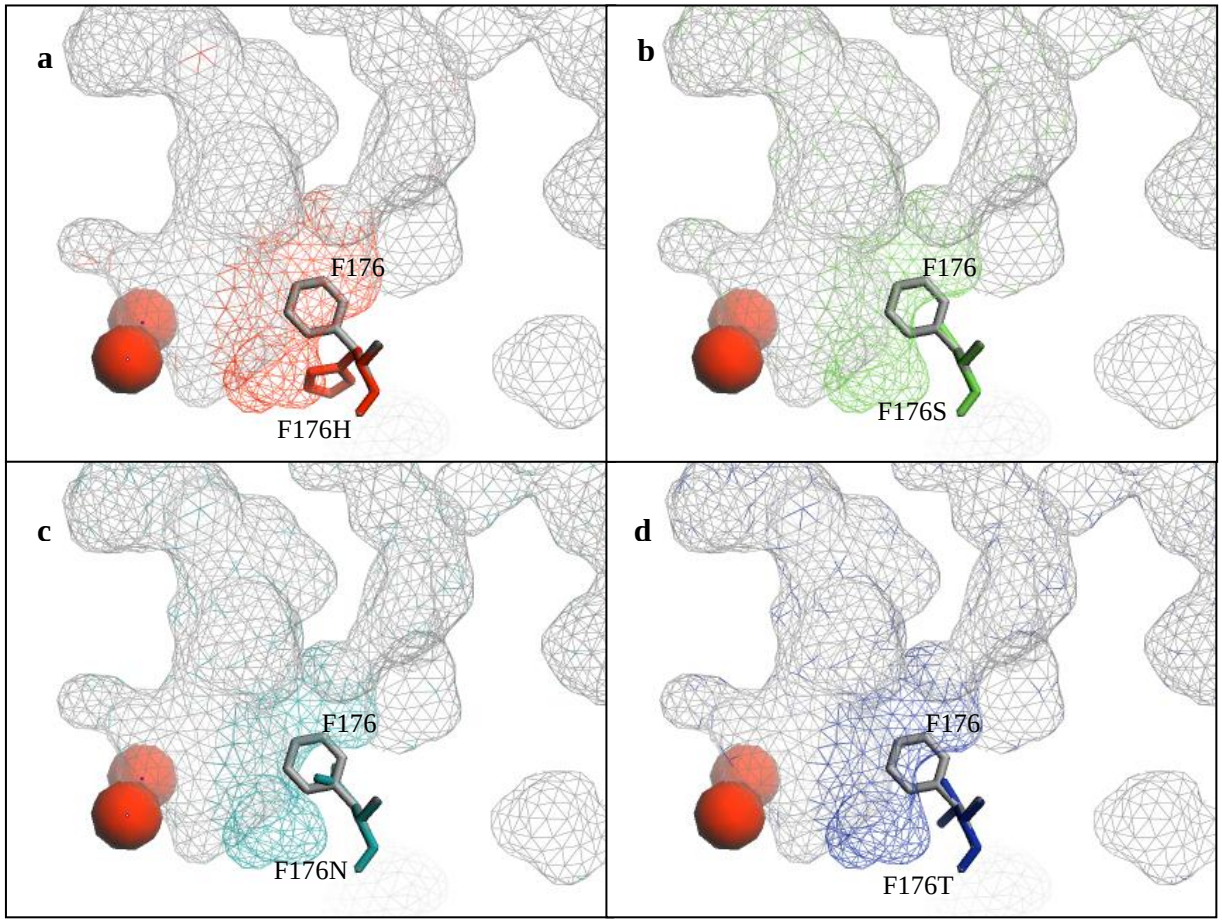

Figure 4.1 Structural alignments of mutant side chains to phenylalanine at TouA 176 and their contributions to hydrophobic cavities: (a) histidine substitution at F176 (red sticks), (b) serine substitution at F176 (green sticks), (c) asparagine substitution at F176 (cyan sticks), (d) theroine substitution at F176 (blue sticks). Wild-type phenylalanine at 176 is shown as gray sticks, iron atoms are red spheres and hydrophobic cavities are as mesh view.

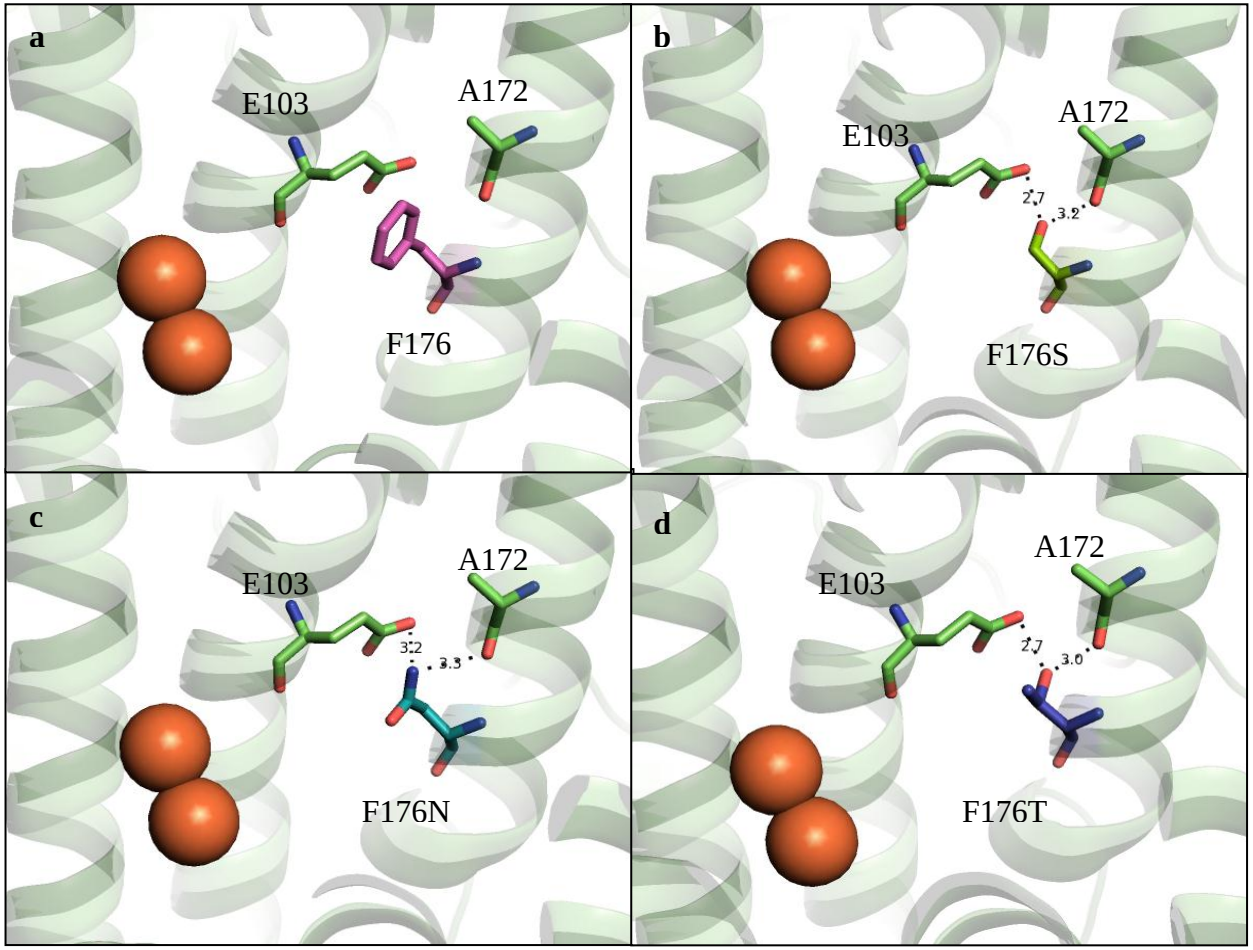

Figure 4.2 H-bonding interactions of TouA F176 mutants with E103 and A172: (a) no H-bonding in wild-type phenylalanine (purple sticks), (b-d) H- bondings by substitutions to serine (green sticks), asparagine (cyan sticks) and threonine (blue sticks) are shown as dots. Oxygen and nitrogen atoms are shown as red and blue and iron atoms are red spheres.

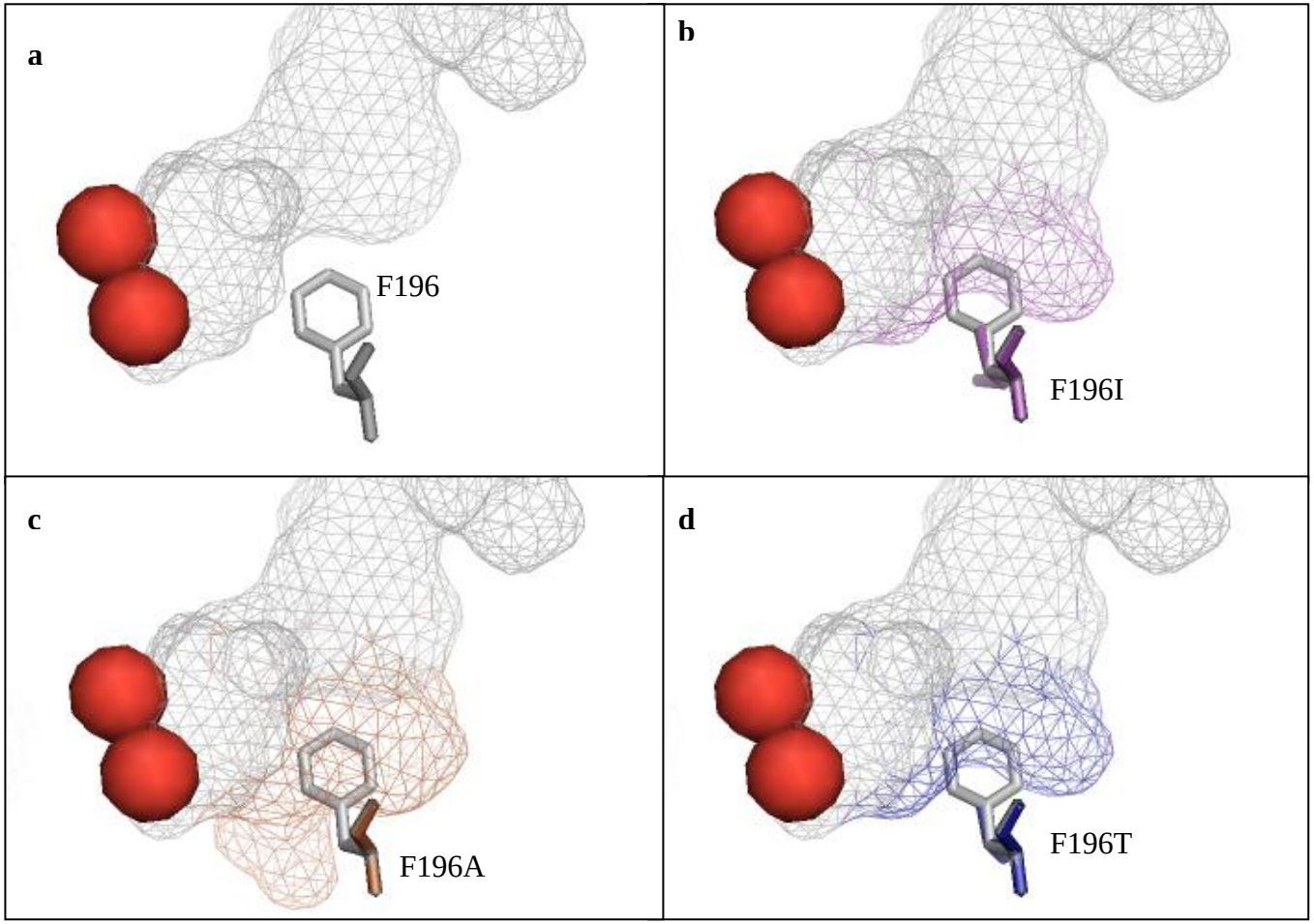

Figure 4.3 Structural alignments of selected mutant side chains to glutamine TouA 196 and their contributions to hydrophobic cavities (a) wild-type phenylalanine at F196 (gray sticks), (b) isoleucine substitution at F196 (purple sticks), (c) alanine substitution at F196 (brown sticks), (d) threonine substitution at F196 (blue sticks). Hydrophobic cavity is shown as mesh view and iron atoms are red spheres.

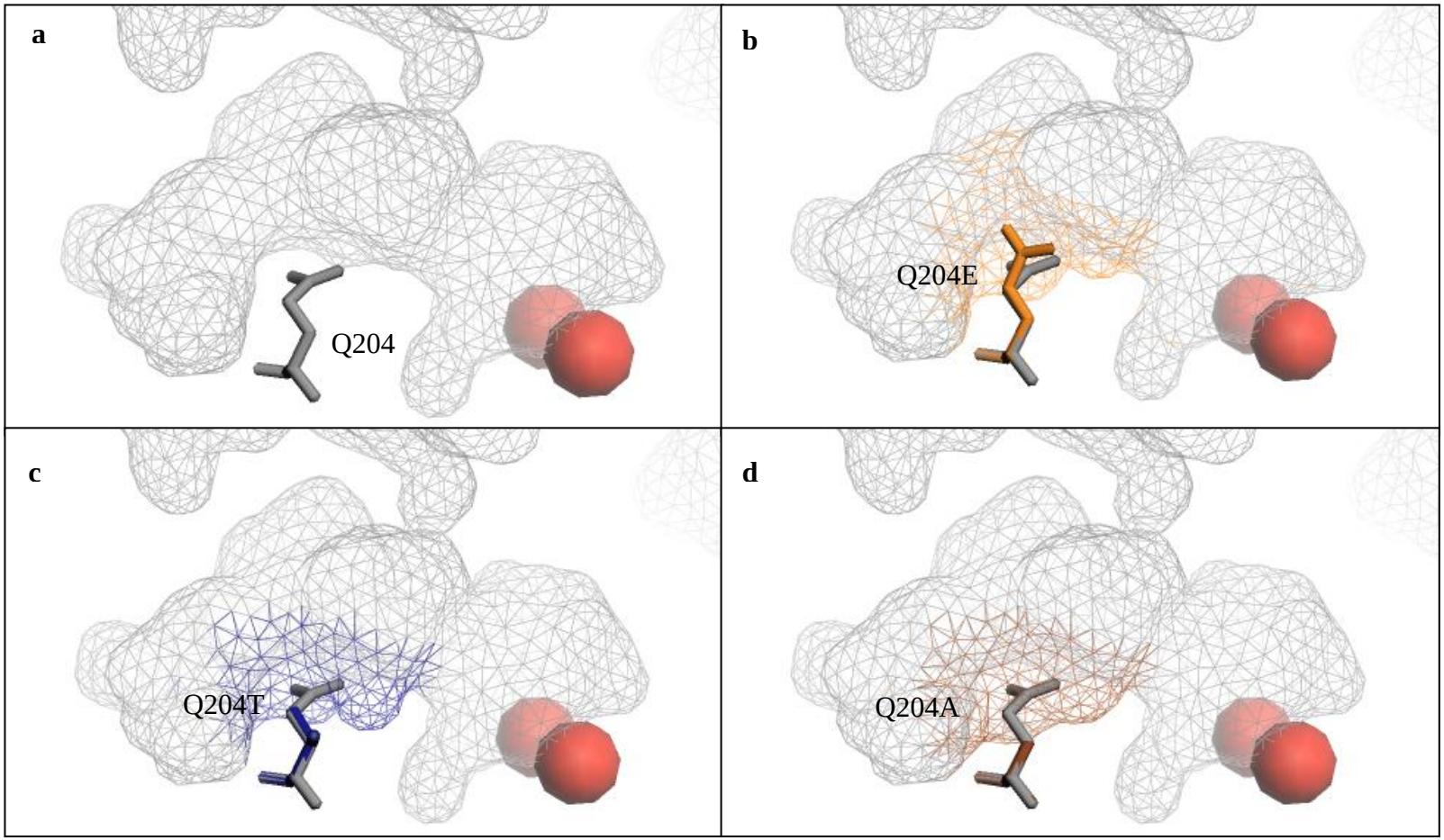

Figure 4.4 Structural alignments of selected mutant side chains to glutamine TouA 204 and their contributions to hydrophobic cavities: (a) wild-type glutamine at Q204 (gray sticks), (b) glutamate substitution at Q204 (orange sticks), (c) threonine substitution at Q204 (blue sticks), (d) alanine substitution at Q204 (brown sticks). Hydrophobic cavity is shown as mesh view and iron atoms are red spheres.

CHAPTER 5

CONCLUSIONS

Site-saturation mutagenesis has enabled us to explore the effect of different substitutions of TouA F176 and F196, two residues at the entrance of substrate binding cavity, and TouA Q204, a residue located on the substrate channel, on the regiospecific oxidation of aromatics. TouA F196 and Q204 have not been studied before and TouA F176 has been investigated by rational design and not by site-saturation mutagenesis. Overall, the mutagenesis yielded both conservative and non-conservative substitutions and effect of the mutations might be substrate dependent.

The site-saturation mutagenesis of TouA F176 position uncovered F176N and F176H substitutions which have not been predicted by rational design before, and the latter was a possible improved mutant for the tested substrates. The substitution of phenylalanine to polar amino acids yielded a more *para*-acting enzyme and TouA F176N was the most regiospecific mutant obtained in this study. Therefore, the results have shown that TouA F176 position affects regiospecificity and activity. TouA F176H mutation may be combined to other reported beneficial mutations to have a more powerful enzyme in the future.

TouA F196, similar to TouA F176 position, is in close proximity to diiron center and might be expected to affect regiospecificity. In addition, the TouA F196 mutant library contained colonies with differing shades of blue (indigo) color. However, there were slight changes in the regiospecificity among TouA F196 variants for the tested substrates. In general, TouA F196 could accommodate various substitutions and retained wild-type level activity, but TouA F196V was not preferred for the oxidation of the tested substrates. The role of this position may be substrate-dependent and the work may be extended to study oxidation of other aromatic compounds in the future.

The substitution of the polar uncharged glutamine at TouA 204 position to a negatively charged glutamate impaired the activity towards all the tested substrates. Hence, a negative charge at this position of substrate channel may not be favored. There was a slight change of the regiospecificity among the TouA Q204 mutants. This position may not have a limited role in the regiospecificity due to its distance from active site; however the tested substrate range can be further broadened as a future work.

APPENDIX A

CALIBRATION CURVES

Authentic chemicals were purchased and analyzed by HPLC to determine the retention times and maximum absorbance wavelengths of each compound to identify products and prepare their calibration curves.

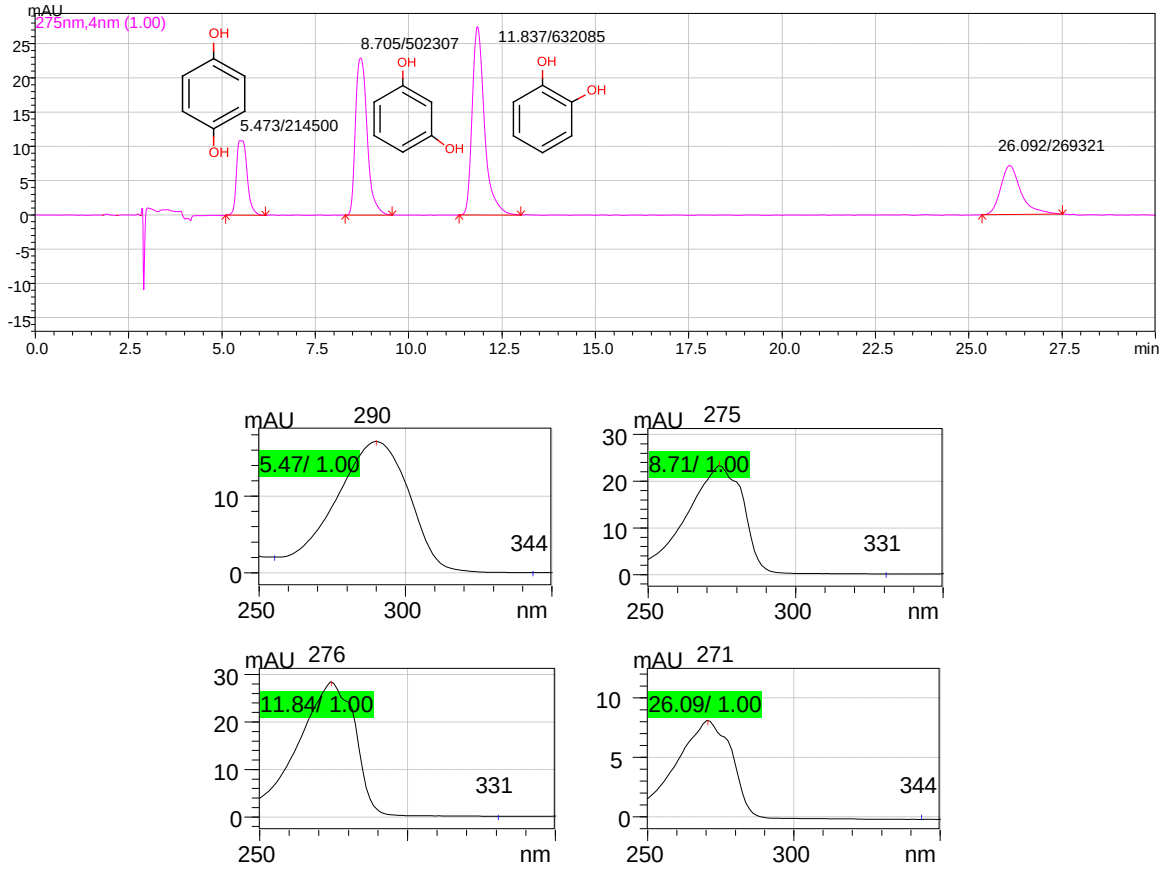

Figure A.1 HPLC chromatogram and maximum absorption wavelengths of standards for identification of products from phenol. Hydroquinone at 5.47 min, 290nm; resorcinol at 8.71 min, 275 nm; catechol at 11.84 min, 275 nm.

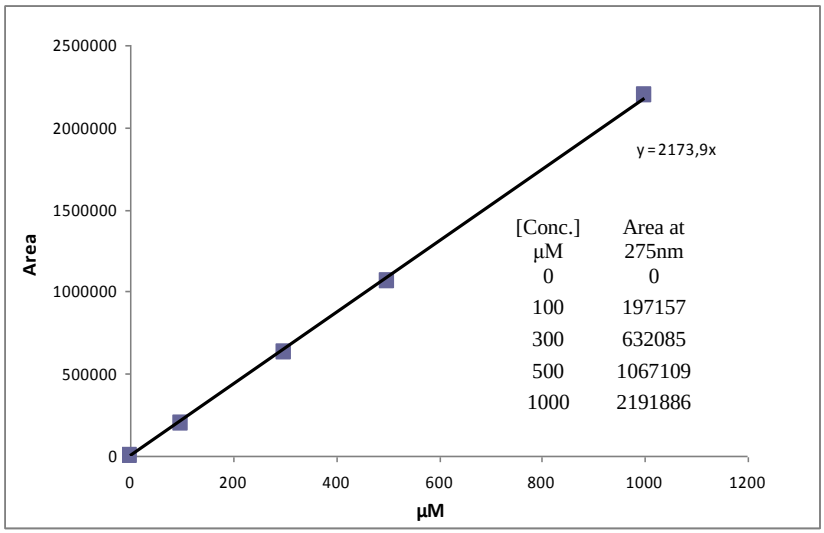

Figure A.2 Standard calibration curve of catechol. Solutions with known concentrations of catechol are analyzed via HPLC and peak areas at 275 nm were derived from the HPLC chromatograms.

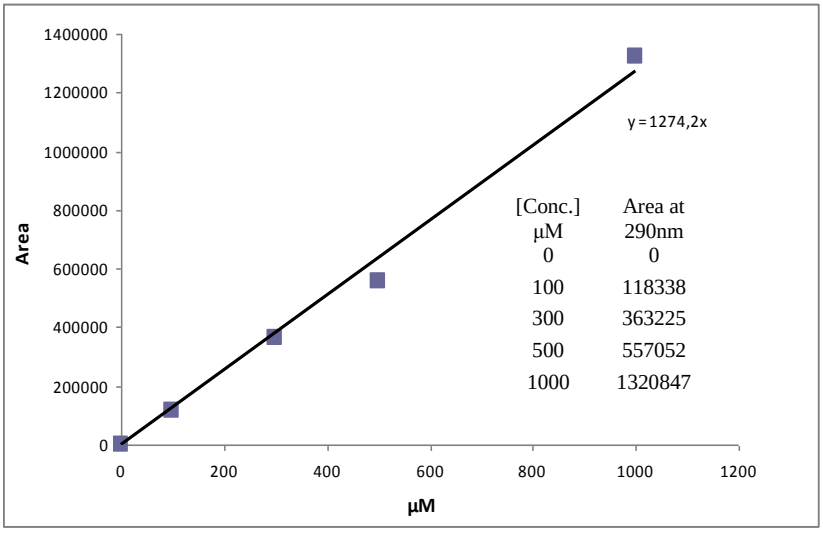

Figure A.3 Standard calibration curve of hydroquinone. Solutions with known concentrations of hydroquinone are analyzed via HPLC and peak areas at 290 nm were derived from the HPLC chromatograms.

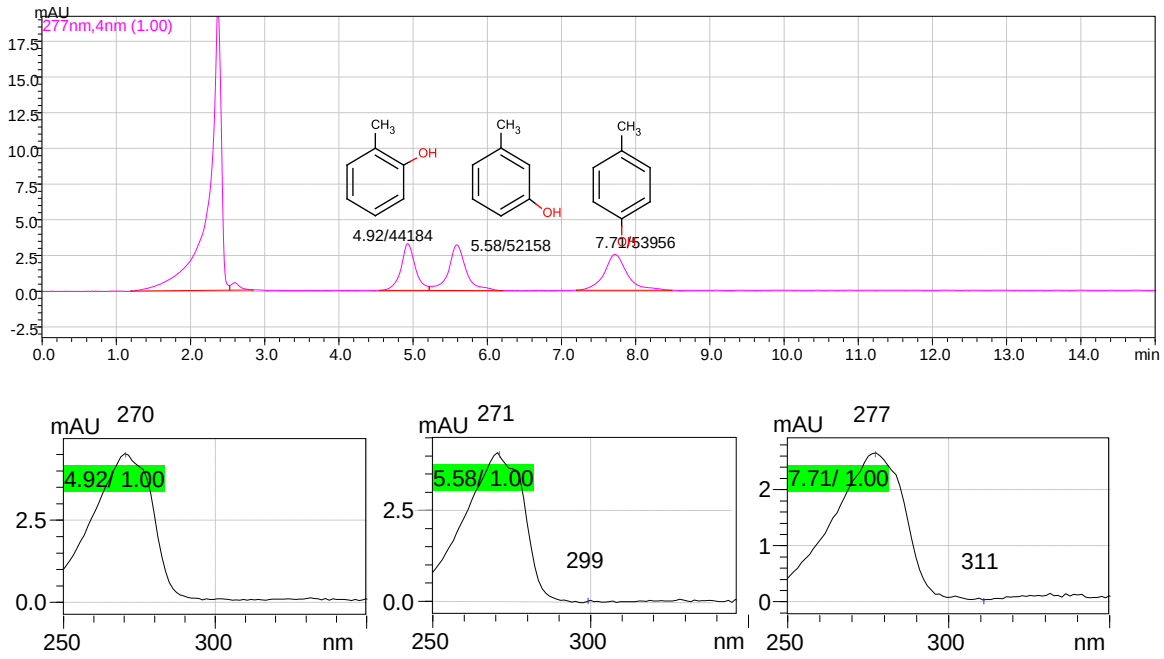

Figure A.4 HPLC chromatogram and maximum absorption wavelengths of standards for identification of products from toluene. *o*-cresol at 4.92 min, 270nm; *p*-cresol at 5.58 min, 270 nm; *m*-cresol at 7.71 min, 277 nm.

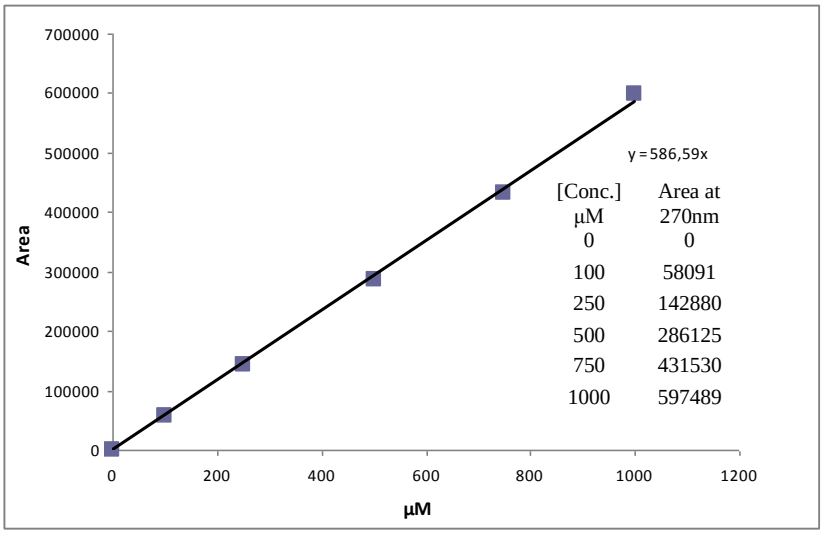

Figure A.5 Standard calibration curve of *o*-cresol. Solutions with known concentrations of *o*-cresol are analyzed via HPLC and peak areas at 270 nm were derived from the HPLC chromatograms.

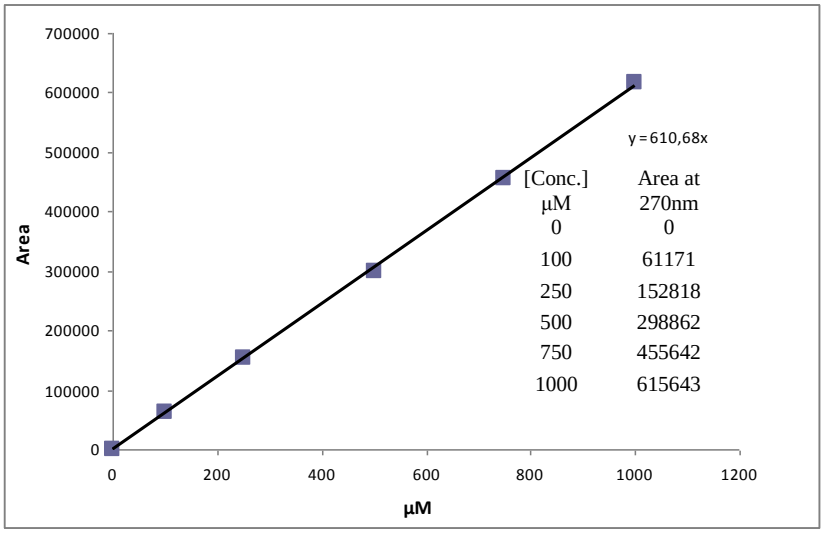

Figure A.6 Standard calibration curve of *m*-cresol. Solutions with known concentrations of *m*-cresol are analyzed via HPLC and peak areas at 270 nm were derived from the HPLC chromatograms.

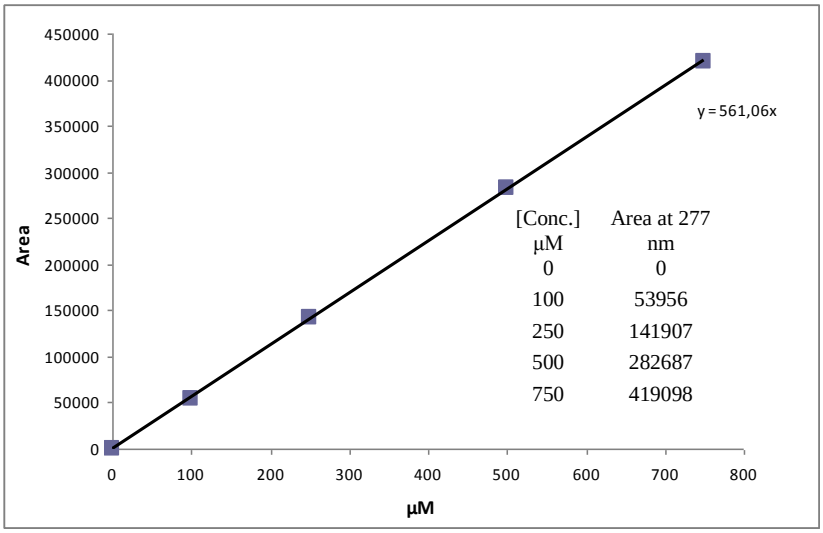

Figure A.7 Standard calibration curve of *p*-cresol. Solutions with known concentrations of *p*-cresol are analyzed via HPLC and peak areas at 277 nm were derived from the HPLC chromatograms.

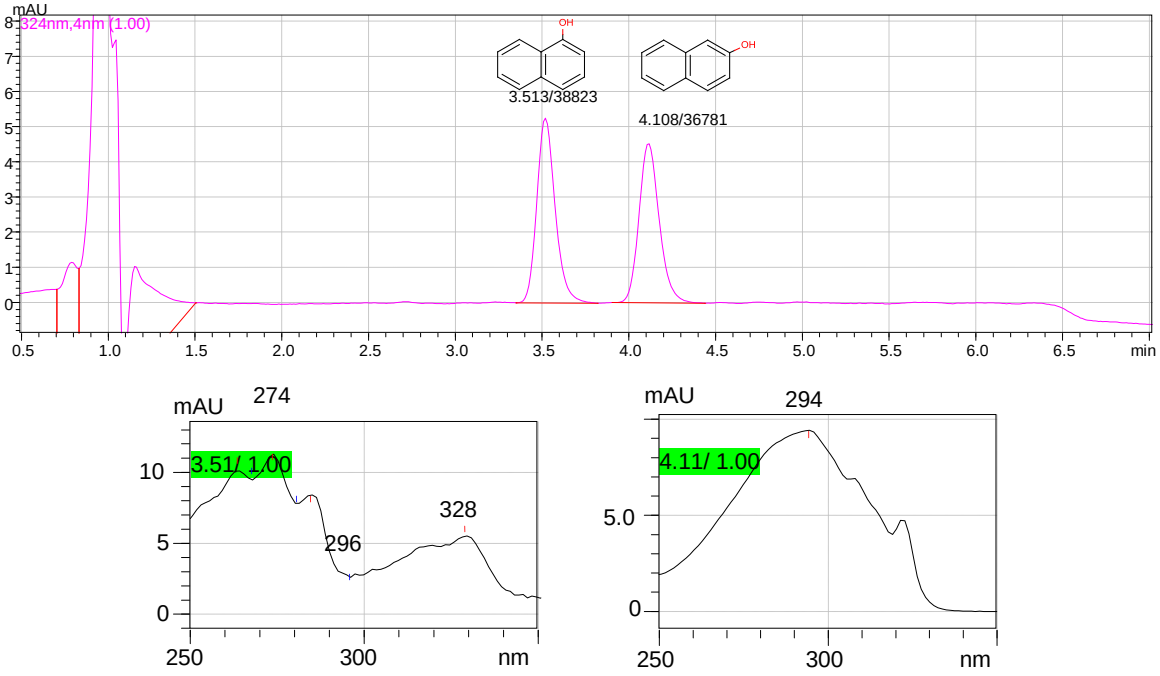

Figure A.8 HPLC chromatogram and maximum absorption wavelengths of standards for identification of products from naphthalene. 1-naphtol is at 3.51 min, 274 nm and 2-naphthol at 4.11 min, 294 nm.

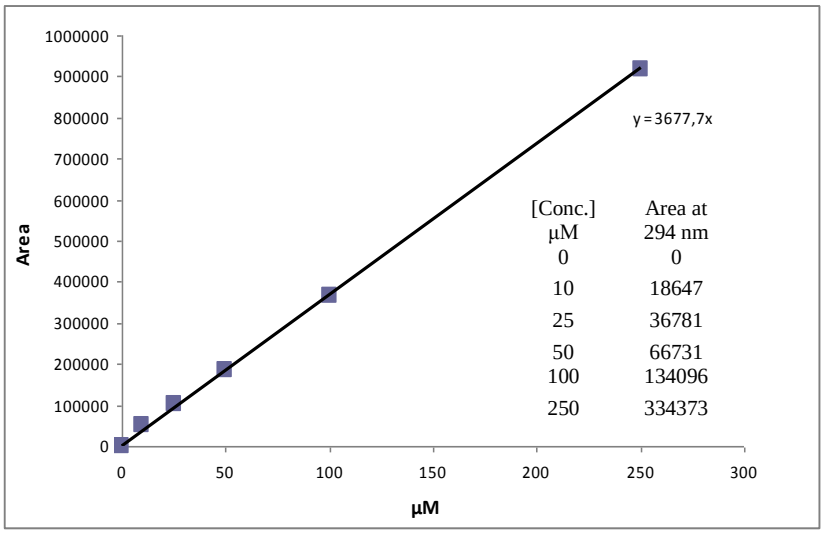

Figure A.9 Standard calibration curve of 1-naphthol. Solutions with known concentrations of 1-naphthol are analyzed via HPLC and peak areas at 294 nm were derived from the HPLC chromatograms.

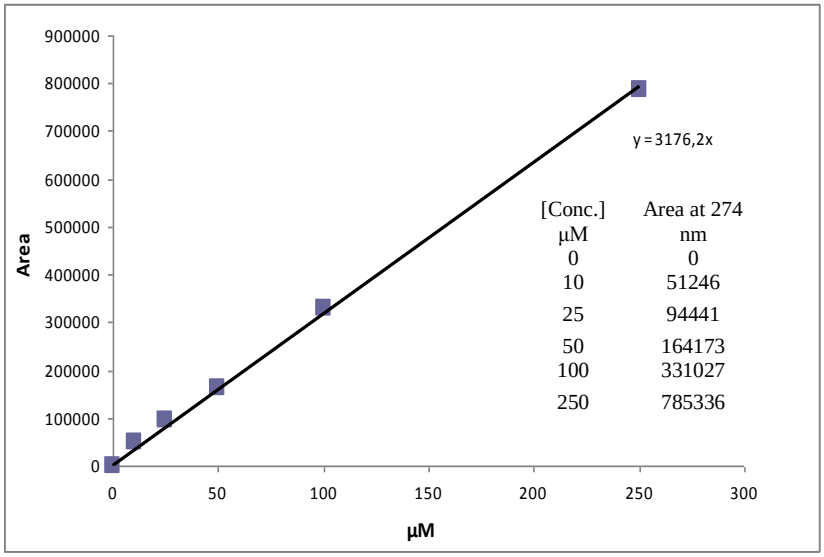

Figure A.10 Standard calibration curve of 2-naphthol. Solutions with known concentrations of 2-naphthol are analyzed via HPLC and peak areas at 274 nm were derived from the HPLC chromatograms.

The activity of *E. coli* TG1/pBS(Kan)ToMO expressing wild-type ToMO and TouA F176, F196 and Q204 variants were presented as the sum of product formation rates from phenol (0.8 mM), toluene (0.25 mM) and naphthalene (5 mM). The initial formation rates were calculated by using at least 3-data points obtained by HPLC analysis of time-course experiments. HPLC peak areas were converted to concentration by referring to standard calibration curves of each product. Concentration of product formed was plotted against time and the slope was derived. The protein content was 0.11 mg protein/ ml per OD_{600}. From the slope and the biomass of each experiment initial formation rates were calculated in nanomoles per minute per milligram of protein for the given concentration of substrates.

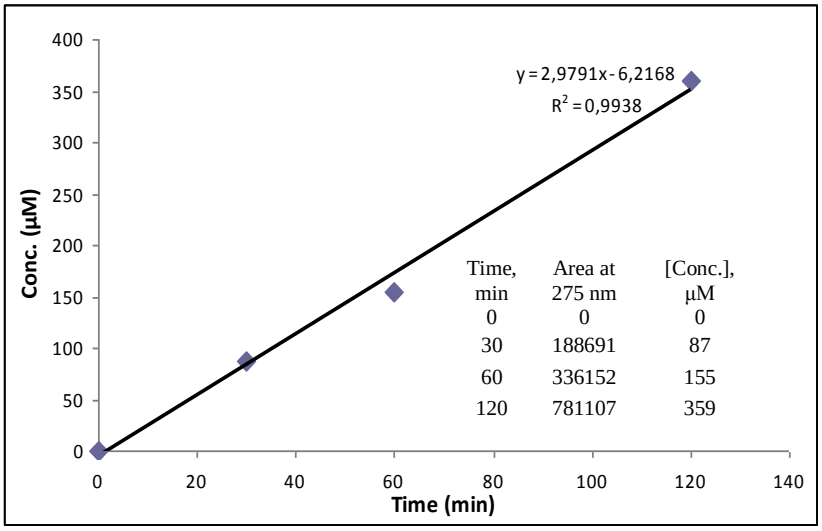

Figure A.11 Representative time-course experiment for catechol formation from phenol by *E. coli* TG1 expressing TouA F196H mutant. For each data point catechol peak area at 275 nm was derived from HPLC chromatograms.

APPENDIX B

LIST of CHEMICALS

1,2-Dihydroxybenzene (Catechol)	Sigma-ALDRICH, Germany
1-Naphthol	MERCK, Germany
2-Naphthol	MERCK, Germany
2-Nitrophenol	Sigma-ALDRICH, Germany
3-Nitrophenol	Sigma-ALDRICH, Germany
4-Nitrocatechol	Sigma-ALDRICH, Germany
4-Nitrophenol >99%	Sigma-ALDRICH, Germany
Acetic acid (glacial) 100%	MERCK, Germany
Acetonitrile	MERCK, Germany
Acrylamide/Bis solution (30%)	Bio-Rad, USA
Agarose Low Melt	AppliChem, Germany
Ammonium iron (III) sulfate dodecahydrate	MERCK Germany
Ammonium per sulfate	Sigma-ALDRICH, Germany
Benzene	MERCK, Germany
Coomassie Brilliant Blue R-250 Bio-Rad USA	Bio-Rad, USA
Ethanol 96%	MERCK, Germany
Ethanol absolute	MERCK, Germany
Ethidium Bromide	Sigma-ALDRICH, Germany
Ethylenediaminetetraacetic acid disodium salt	Carlo ERBA Italy
Formic acid (98-100%)	MERCK, Germany
Gene Ruler 1 kb DNA Ladder	Fermentas, USA
Glycerol anhydrous	AppliChem, Germany
Glycine	MERCK, Germany
Hydrochloric acid (HCl)	MERCK, Germany
Hydroquinone	Sigma-ALDRICH, Germany
Kanamycin sulfate	AppliChem, Germany
LB-Agar (MILLER)	MERCK, Germany
LB-Broth (MILLER)	MERCK, Germany
m-Cresol	Sigma-ALDRICH, Germany

Methanol for liquid chromatography	MERCK, Germany
N, N-Dimethyl-formamide (DMF)	MERCK, Germany
Naphthalene MERCK Germany	Carlo ERBA, Italy
Nitric acid fuming 100% extra pure	MERCK, Germany
Nitrobenzene >=99%	Sigma-ALDRICH, Germany
o-Cresol	Sigma-ALDRICH, Germany
p-Cresol	Sigma-ALDRICH, Germany
Phenol kristallin	AppliChem, Germany
p-Nitrophenol	Carlo ERBA, Italy
Protein Ladder, PageRuler+Prestained, 26619	Pierce, USA
Resorcinol (1,3-Benzenediol)	Sigma-ALDRICH, Germany
SDS	MERCK, Germany
SDS loading buffer pack	Fermentas, USA
Sodium acetate anhydrous	AppliChem, Germany
Sodium Chloride	MERCK, Germany
Sodium Hydroxide pellets	MERCK, Germany
TEMED	BIOMATIK, USA
Toluene (extra pure)	Riedel de Haen, Germany
Tris (hydroxymethyl)-aminomethane	MERCK, Germany

REFERENCES

Agency for Toxic Substances and Disease Registry (ATSDR), *Toxicological Profile for Nitroenzene*, CAS No. 98-95-3, Atlanta, 1990.

Agency for Toxic Substances and Disease Registry (ATSDR), *Toxicological Profile for Toluene*. CAS No. 108-88-3, Atlanta, 2000.

Agency for Toxic Substances and Disease Registry (ATSDR), *Toxicological Profile for Cresols*, CAS No. 1319-77-3, Atlanta, 2008a.

Agency for Toxic Substances and Disease Registry (ATSDR), *Toxicological Profile for Phenol*, CAS No. 108-95-2, Atlanta, 2008b.

Agency for Toxic Substances and Disease Registry (ATSDR), *Toxicological Profile for Benzene*, CAS No. 71-43-2 Atlanta, 2007.

United States Environmental Protection Agency (EPA), *Technology Transfer Network Air Toxics Web Site*, 2007, http://www.epa.gov/ttn/atw/hlthef/pyrocate.html

Alvarez-Cohen, L. and McCarty, P. L., "Product Toxicity and Cometabolic Competitive Inhibition Modeling of Chloroform and Trichloroethylene Transformation by Methanotrophic Resting Cells", *Applied Environmental Microbiology*, Vol. 57, pp. 1031-1037, 1991.

Arnold, F. H., "Design by Directed Evolution", *Faseb Journal* , Vol. 11, pp. A872-A872, 1997.

Baggi, G., Barbieri, P., Galli, E. and Tollari, S., "Isolation of a Pseudomonas Stutzeri Strain That Degrades *o*-Xylene", *Applied Environmental Microbiology*, Vol. 53, pp. 2129-2132, 1987.

Bailey, L. J., McCoy, J. G., Phillips, G. N. and Fox, B. G., "Structural Consequences of Effector Protein Complex Formation in a Diiron Hydroxylase", *Proceedings of the National Academy of Sciences of the United States of America*, Vol. 105, pp. 19194-19198, 2008.

Baldwin, B. R., Nakatsu, C. H., Nebe, J., Wickham, G. S., Parks, C. and Nies, L., "Enumeration of Aromatic Oxygenase Genes to Evaluate Biodegradation During Multi-Phase Extraction at a Gasoline-Contaminated Site", *Journal of Hazardous Materials*, Vol. 163, pp. 524-530, 2009

Bertoni, G., Martino, M., Galli, E. and Barbieri, P., "Analysis of the Gene Cluster Encoding Toluene/*o*-Xylene Monooxygenase from Pseudomonas Stutzeri Ox1", *Applied and Environmental Microbiology*,Vol. 64, pp, 3626-3632, 1998.

Bochevarov, A. D., Li, J. N., Song, W. J., Friesner, R. A. and Lippard, S. J., "Insights into the Different Dioxygen Activation Pathways of Methane and Toluene Monooxygenase Hydroxylases", *Journal of the American Chemical Society*, Vol. 133, pp. 7384-7397, 2011.

Bommarius, A. S., Blum, J. K. and Abrahamson, M. J., "Status of Protein Engineering for Biocatalysts: How to Design an Industrially Useful Biocatalyst", *Current Opinion in Chemical Biology*, Vol. 15, pp. 194-200, 2011.

Bonifacio, M. J., Palma, P. N., Almeida, L. and Soares-Da-Silva, P., "Catechol-*O*-Methyltransferase and Its Inhibitors in Parkinson's Disease", *Cns Drug Reviews*, Vol. 13, pp. 352-379, 2007.

Bornscheuer, U. T., Huisman, G. W., Kazlauskas, R. J., Lutz, S., Moore, J. C. and Robins, K., "Engineering the Third Wave of Biocatalysis", *Nature*, Vol. 485, pp. 185-194, 2012.

Bornscheuer, U. T. and Pohl, M., "Improved Biocatalysts by Directed Evolution and Rational Protein Design", *Current Opinion in Chemical Biology*, Vol. 5, pp. 137-143, 2001.

Bouwer, E. J. and Zehnder, A. J.,"Bioremediation of Organic Compounds-Putting Microbial Metabolism to Work", *Trends Biotechnology*, Vol. 11, pp. 360-367, 1993.

Bradley, P. M. and Chapelle, F. H., "Effect of Contaminant Concentration on Aerobic Microbial Mineralization of Dce and Vc in Stream-Bed Sediments", *Environmental Science & Technology*, Vol. 32, pp. 553-357, 1998.

Buchman, J. S., Schneider, K. D., Lloyd, A. R., Pavlish, S. L. and Leonard, D. A., "Site-Saturation Mutagenesis of Position V117 in Oxa-1 Beta-Lactamase: Effect of Side Chain Polarity on Enzyme Carboxylation and Substrate Turnover", *Biochemistry*, Vol. 51, pp. 3143-3150, 2012.

Byrne, A. M., Kukor, J. J. and Olsen, R. H., "Sequence Analysis of the Gene Cluster Encoding Toluene-3-Monooxygenase from Pseudomonas Pickettii Pko1", *Gene*, Vol. 154, pp. 65-70, 1995.

Cafaro, V., Notomista, Capasso, E. P. and Di Donato, A., "Mutation of Glutamic Acid 103 of Toluene O-Xylene Monooxygenase as a Means to Control the Catabolic Efficiency of a Recombinant Upper Pathway for Degradation of Methylated Aromatic Compounds", *Applied and Environmental Microbiology*, Vol. 71, pp. 4744-4750, 2005.

Cafaro, V., Scognamiglio, R., Viggiani, A., Izzo, V., Passaro, I., Notomista, E., Dal Piaz, F., Amoresano, A., Casbarra, A., Pucci, P. and Di Donato. A., "Expression and Purification of the Recombinant Subunits of Toluene/O-Xylene Monooxygenase and Reconstitution of the Active Complex", *European Journal of Biochemistry*, Vol. 269, pp. 5689-5699, 2002.

Chauhan, S., Barbieri, P. and Wood, T. K., "Oxidation of Trichloroethylene, 1,1-Dichloroethylene, and Chloroform by Toluene/O-Xylene Monooxygenase from Pseudomonas Stutzeri Ox1", *Applied and Environmental Microbiology*, Vol. 64, pp. 3023-3024, 1998.

Chen, W., Bruhlmann, F., Richins, R. D. and Mulchandani, A., "Engineering of Improved Microbes and Enzymes for Bioremediation", *Current Opinion in Biotechnology*, Vol. 10, pp. 137-141, 1999.

Chica, R. A., Doucet, N. and Pelletier, J. N., "Semi-rational approaches to engineering enzyme activity: combining the benefits of directed evolution and rational design", *Current Opinion in Biotechnology*, Vol:16(4), pp. 378-384, 2005.

Cohen, N., Abramov, S., Dror, Y. and Freeman, A., "In Vitro Enzyme Evolution: The Screening Challenge of Isolating the One in a Million", *Trends in Biotechnology*, Vol. 19, pp. 507-510, 2001.

Crameri, A., Raillard, S. A., Bermudez, E. and Stemmer. W. P. C., "Dna Shuffling of a Family of Genes from Diverse Species Accelerates Directed Evolution", *Nature*, Vol. 391, pp. 288-291, 1998.

de Carvalho, C. C. C. R., "Enzymatic and Whole Cell Catalysis: Finding New Strategies for Old Processes", *Biotechnology Advances*, Vol. 29, pp. 75-83, 2011.

Dietrich, M., Do, T. A., Schmid, R. D., Pleiss, J. and Urlacher, V. B., "Altering the Regioselectivity of the Subterminal Fatty Acid Hydroxylase P450 Bm-3 Towards Gamma- and Delta-Positions", *Journal of Biotechnology*, Vol. 139, pp. 115-117, 2009.

Fishman, A., Tao, Y., Rui, L. Y. and Wood, T. K., "Controlling the Regiospecific Oxidation of Aromatics Via Active Site Engineering of Toluene Para-Monooxygenase of Ralstonia Pickettii Pko1", *Journal of Biological Chemistry*, Vol. 280, pp. 506-14, 2005.

Fishman, A., Tao, Y. Vardar, G. and Wood, T. K., "Controlling Regiospecific Oxidation of Aromatics and the Degradation of Chlorinated Aliphatics via Active Site Engineering of Toluene Monooxygenases" in Ramos, J. L. and Levesque R., (Eds.), *Pseudomonas*, pp. 237-286, Springer, Netherlands, 2006.

Ho, S. N. Hunt, H. D., Horton, R. M., Pullen, J. K. and Pease, L. R., "Site-Directed Mutagenesis by Overlap Extension Using the Polymerase Chain Reaction",*Gene*, Vol. 77, pp. 51-59, 1989.

Ju, K. S. and Parales, R. E., "Control of Substrate Specificity by Active-Site Residues in Nitrobenzene Dioxygenase", *Applied and Environmental Microbiology*, Vol. 72, pp. 1817-1824, 2006.

Ma, Y. and Herson, D. S., "The Catechol 2,3-Dioxygenase Gene and Toluene Monooxygenase Genes from Burkholderia Sp Aa1, an Isolate Capable of Degrading Aliphatic Hydrocarbons and Toluene", *Journal of Industrial Microbiology & Biotechnology*, Vol. 25, pp. 127-31, 2000.

McClay, K., Boss, C., Keresztes, I. and Steffan, R. J., "Mutations of Toluene-4-Monooxygenase That Alter Regiospecificity of Indole Oxidation and Lead to Production of Novel Indigoid Pigments", *Applied and Environmental Microbiology*, Vol. 71, pp. 5476-5483, 2005.

McCormick, M. S. and Lippard., S. J., "Analysis of Substrate Access to Active Sites in Bacterial Multicomponent Monooxygenase Hydroxylases: X-Ray Crystal Structure of Xenon-Pressurized Phenol Hydroxylase from Pseudomonas Sp. Ox1", *Biochemistry*, Vol. 50, pp. 11058-11069, 2011.

McCormick, M. S., Sazinsky, M. H., Condon, K. L. and Lippard, S. J., "X-Ray Crystal Structures of Manganese(II)-Reconstituted and Native Toluene/O-Xylene Monooxygenase Hydroxylase Reveal Rotamer Shifts in Conserved Residues and an Enhanced View of the Protein Interior" *Journal of the American Chemical Society*, Vol. 128, pp. 15108-15110, 2006.

Meyer, H. P. and Turner, N. J., "Biotechnological Manufacturing Options for Organic Chemistry", *Mini-Reviews in Organic Chemistry*, Vol. 6, pp. 300-306, 2009.

Mithaishvili, T., Scalla, R., Ugrekhelidze, D., Tsereteli, B., Sadunishvili, T. and Kvesitadze, G., "Degradation of Aromatic Compounds in Plants Grown under Aseptic Conditions", *Zeitschrift Fur Naturforschung C*, Vol. 60, pp. 97-102, 2005.

Murray, L. J. and Lippard, S. J., "Substrate Trafficking and Dioxygen Activation in Bacterial Multicomponent Monooxygenases", *Accounts of Chemical Research*, Vol. 40, pp. 466-474, 2007.

Nebe, J., Baldwin, B. R., Kassab, R. L., Nies, L. and Nakatsu, C. H., "Quantification of Aromatic Oxygenase Genes to Evaluate Enhanced Bioremediation by Oxygen Releasing Materials at a Gasoline-Contaminated Site", *Environmental Science & Technology*, Vol. 43, pp. 2029-2034, 2009.

Newman, L. M. and Wackett, L. P., "Purification and Characterization of Toluene 2-Monooxygenase from Burkholderia Cepacia G4", *Biochemistry*, Vol. 34, pp. 14066-14076, 1995.

Notomista, E., Cafaro, V., Bozza, G. and Di Donato, A., "Molecular Determinants of the Regioselectivity of Toluene/*o*-Xylene Monooxygenase from Pseudomonas Sp Strain Ox1", *Applied and Environmental Microbiology*, Vol. 75, pp. 823-836, 2009.

Notomista, E., Lahm, A., Di Donato, A. and Tramontano, A., "Evolution of Bacterial and Archaeal Multicomponent Monooxygenases", *Journal of Molecular Evolution*, Vol. 56, pp. 435-445, 2003.

Notomista, E., Scognamiglio, R., Troncone, L., Donadio, G., Pezzella, A., Di Donato, A. and Izzo, V., "Tuning the Specificity of the Recombinant Multicomponent Toluene O-Xylene Monooxygenase from Pseudomonas Sp Strain Ox1 for the Biosynthesis of Tyrosol from 2-Phenylethanol", *Applied and Environmental Microbiology*, Vol. 77, pp. 5428-5437, 2011.

Palma, P. N., Bonifacio, M. J., Loureiro, A. I., Wright, L. C., Learmonth, D. A. and Soares-da-Silva, P., "Molecular Modeling and Metabolic Studies of the Interaction of Catechol-O-Methyltransferase and a New Nitrocatechol Inhibitor", *Drug Metabolism and Disposition*, Vol. 31, pp. 250-258, 2003.

Palumbo, A., Napolitano, A. and d'Ischia, M., "Nitrocatechols Versus Nitro Catecholamines as Novel Competitive Inhibitors of Neuronal Nitric Oxide Synthase: Lack of the Aminoethyl Side Chain Determines Loss of Tetrahydrobiopterin-Antagonizing Properties", *Bioorganic & Medicinal Chemistry Letters*, Vol. 12, pp. 13-16, 2002.

Radice, F., Orlandi, V., Massa, V., Cavalca, L., Demarta, A., Wood, T. K. and Barbieri, P., "Genotypic Characterization and Phylogenetic Relations of Pseudomonas Sp (Formerly P-Stutzeri) Ox1", *Current Microbiology*, Vol. 52, pp. 395-399, 2006.

Raynaudlacroze, P. O. and Tavare, N. S., "Separation of 2-Naphthol - Hydrotropy and Precipitation", *Industrial & Engineering Chemistry Research*, Vol. 32, pp. 685-691, 1993.

Rubin-Pitel, S. B. and Zhao, H. M., "Recent Advances in Biocatalysis by Directed Enzyme Evolution", *Combinatorial Chemistry & High Throughput Screening*, Vol. 9, pp. 247-257, 2006.

Rui, L. Y., Reardon, K. F. and Wood, T. K., "Protein engineering of toluene ortho-monooxygenase of Burkholderia cepacia G4 for regiospecific hydroxylation of indole to form various indigoid compounds", *Applied Microbiology and Biotechnology*, Vol: 66(4), pp. 422-429, 2005.

Rui, L. Y., Kwon, Y. M., Fishman, A., Reardon, K. F. and Wood, T. K., "Saturation Mutagenesis of Toluene Ortho-Monooxygenase of Burkholderia Cepacia G4 for Enhanced 1-Naphthol Synthesis and Chloroform Degradation", *Applied and Environmental Microbiology*, Vol. 70, pp. 3246-3252, 2004.

Ryoo, D., Shim, H., Arenghi, F. L. G., Barbieri, P. and Wood, T. K., "Tetrachloroethylene, Trichloroethylene, and Chlorinated Phenols Induce Toluene-O-Xylene Monooxygenase Activity in Pseudomonas Stutzeri Ox1", *Applied Microbiology and Biotechnology*, Vol. 56, pp. 545-549, 2001.

Ryoo, D., Shim, H., Canada, K., Barbieri, P. and Wood, T. K., "Aerobic Degradation of Tetrachloroethylene by Toluene-O-Xylene Monooxygenase of Pseudomonas Stutzeri Ox1", *Nature Biotechnology*, Vol. 18, pp. 775-78, 2000.

Sazinsky, M. H., Bard, J., Di Donato, A. and Lippard, S. J., "Crystal Structure of the Toluene/*o*-Xylene Monooxygenase Hydroxylase from Pseudomonas Stutzeri Ox1 - Insight into the Substrate Specificity, Substrate Channeling, and Active Site Tuning of Multicomponent Monooxygenases", *Journal of Biological Chemistry*, Vol. 279, pp. 30600-30610, 2004.

Sazinsky, M. H. and Lippard, S. J., "Correlating Structure with Function in Bacterial Multicomponent Monooxygenases and Related Diiron Proteins", *Accounts of Chemical Research*, Vol. 39, pp. 558-566, 2006.

Shim, H. J. and Wood, T. K., "Aerobic Degradation of Mixtures of Chlorinated Aliphatics by Cloned Toluene-*o*-Xylene Monooxygenase and Toluene O-Monooxygenase in Resting Cells", *Biotechnology and Bioengineering*, Vol. 70, pp. 693-698, 2000.

Shim, H., Ryoo, D., Barbieri, P. and Wood, T. K., "Aerobic Degradation of Mixtures of Tetrachloroethylene, Trichloroethylene, Dichloroethylenes, and Vinyl Chloride by Toluene-O-Xylene Monooxygenase of Pseudomonas Stutzeri Ox1", *Applied Microbiology and Biotechnology*, Vol. 56, pp. 265-69, 2001.

Siani, L., Papa, R., Di Donato, A. and Sannia, G., "Recombinant Expression of Toluene O-Xylene Monooxygenase (Tomo) from Pseudomonas Stutzeri Ox1 in the Marine Antarctic Bacterium Pseudoalteromonas Haloplanktis Tac125", *Journal of Biotechnology*, Vol. 126, pp. 334-341, 2006.

Siloto, R. M. P. and Weselake, R. J., "Site Saturation Mutagenesis: Methods and Applications in Protein Engineering", *Biocatalysis and Agricultural Biotechnology*, Vol 1, pp. 181-189, 2012.

Song, W.J., *Understanding Orchestrated Chemical Teactions in Toluene/o-Xylene from Pseudomonas Sporium OX1*, Ph.D. Thesis, Massachusetts Institute of Technology, 2011.

Song, W. J., Gucinski, G., Sazinsky, M. H. and Lippard, S. J., "Tracking a Defined Route for O-2 Migration in a Dioxygen-Activating Diiron Enzyme", *Proceedings of the National Academy of Sciences of the United States of America*, Vol. 108, pp. 14795-14800, 2011.

Song, W. J., McCormick, M. S., Behan, R. K., Sazinsky, M. H., Jiang, W., Lin, J., Krebs, C. and Lippard, S. J., "Active Site Threonine Facilitates Proton Transfer During Dioxygen Activation at the Diiron Center of Toluene/*o*-Xylene Monooxygenase Hydroxylase", *Journal of the American Chemical Society*, Vol. 132, pp.13582-13585, 2010.

Steffens, D. L. and Williams, J. G., "Efficient site-directed saturation mutagenesis using degenerate oligonucleotides", *Journal of Biomolecular Techiques*, Vol:18(3), pp. 147-149, (2007).

Stemmer, W. P, "DNA Shuffling by Random Fragmentation and Reassembly: In Vitro Recombination for Molecular Evolution", *Proceedings of the National Academy of Sciences of the United States of America*, Vol. 91, pp. 10747-10751, 1994.

Tao, Y., Bentley, W. E. and Wood, T. K., "Regiospecific Oxidation of Naphthalene and Fluorene by Toluene Monooxygenases and Engineered Toluene 4-Monooxygenases of Pseudomonas Mendocina Kr1", *Biotechnology and Bioengineering*, Vol. 90, 85-94, 2005.

Tao, Y., Fishman, A., Bentley, W. E. and Wood, T. K., "Altering Toluene 4-Monooxygenase by Active-Site Engineering for the Synthesis of 3-Methoxycatechol, Methoxyhydroquinone, and Methylhydroquinone", *Journal of Bacteriology*, Vol. 186, pp. 4705-4713, 2004a.

Tao, Y., Fishman, A., Bentley, W. E. and Wood, T. K., "Oxidation of Benzene to Phenol, Catechol, and 1,2,3-Trihydroxybenzene by Toluene 4-Monooxygenase of Pseudomonas Mendocina Kr1 and Toluene 3-Monooxygenase of Ralstonia Pickettii Pko1", *Applied and Environmental Microbiology*, Vol. 70, pp. 3814-3820, 2004b.

The PyMOL Molecular Graphics System, Version 1.5.0.4, Schrödinger, LLC., New York, 2010.

Turner, N. J, "Directed Evolution Drives the Next Generation of Biocatalysts", *Nature Chemical Biology*, Vol. 5, pp. 568-574, 2009.

Vardar, G. and Wood, T. K., "Protein Engineering of Toluene-O-Xylene Monooxygenase from Pseudomonas Stutzeri Ox1 for Synthesizing 4-Methylresorcinol, Methylhydroquinone, and Pyrogallol", *Applied and Environmental Microbiology*, Vol. 70, pp. 3253-3262, 2004.

Vardar, G., Barbieri, P. and T. K., Wood, "Chemotaxis of Pseudomonas Stutzeri Ox1 and Burkholderia Cepacia G4 toward Chlorinated Ethenes", *Applied Microbiology and Biotechnology*, Vol. 66, pp. 696-701, 2005a.

Vardar, G., Ryu, K. and Wood, T. K., "Protein Engineering of Toluene-O-Xylene Monooxygenase from Pseudomonas Stutzeri Ox1 for Oxidizing Nitrobenzene to 3-Nitrocatechol, 4-Nitrocatechol, and Nitrohydroquinone", *Journal of Biotechnology*, Vol. 115, pp. 145-56, 2005b.

Vardar, G., Tao, Y., Lee, J. and Wood, T. K., "Alanine 101 and Alanine 110 of the Alpha Subunit of Pseudomonas Stutzeri Ox1 Toluene-O-Xylene Monooxygenase Influence the Regiospecific Oxidation of Aromatics", *Biotechnology and Bioengineering*, Vol. 92, pp. 652-658, 2005c.

Vardar, G. and Wood, T. K., "Alpha-Subunit Positions Methionine 180 and Glutamate 214 of Pseudomonas Stutzeri Ox1 Toluene-O-Xylene Monooxygenase Influence Catalysis", *Journal of Bacteriology*, Vol. 187, pp. 1511-1514, 2005a.

Vardar, G. and Wood, T. K., "Protein Engineering of Toluene-O-Xylene Monooxygenase from Pseudomonas Stutzeri Ox1 for Enhanced Chlorinated Ethene Degradation and O-Xylene Oxidation", *Applied Microbiology and Biotechnology*, Vol. 68, pp. 510-517, 2005b.

Vidali, M., "Bioremediation. An Overview", *Pure and Applied Chemistry*,Vol. 73, pp. 1163-1172, 2001.

Wood, T. K, "Molecular Approaches in Bioremediation", *Current Opinion in Biotechnology*, Vol. 19, 572-578, 2008.

Yen, K. M., Karl, M. R., Blatt, L. M., Simon, M. J., Winter, R. B., Fausset, P. R., Lu, H. S., Harcourt, A. A. and Chen, K. K., "Cloning and Characterization of a Pseudomonas Mendocina Kr1 Gene Cluster Encoding", *Journal of Bacteriology*, Vol. 173, 5315-5327, 1991.

Zhao, H. M., Chockalingam, K. and Chen, Z. L., "Directed Evolution of Enzymes and Pathways for Industrial Biocatalysis", *Current Opinion in Biotechnology*, Vol. 13, pp. 104-110, 2002.